

# SLIDE: a surrogate fairness constraint to ensure fairness consistency<sup>\*</sup>

Kunwoong Kim<sup>a</sup>, Ilsang Ohn<sup>b,1</sup>, Sara Kim<sup>c,2</sup> and Yongdai Kim<sup>a,\*</sup>

<sup>a</sup>Department of Statistics, Seoul National University, Seoul, 08826, Republic of Korea

<sup>b</sup>Department of Statistics, Inha University, Incheon, 22212, Republic of Korea

<sup>c</sup>Core Technology R&D team, Mechatronic R&D Center, Samsung Electronics, Hwaseong, 18448, Republic of Korea

## ARTICLE INFO

### Keywords:

Fairness AI  
Learning theory  
Machine learning  
Supervised learning  
Classification

## ABSTRACT

As they have a vital effect on social decision makings, AI algorithms should be not only accurate and but also fair. Among various algorithms for fairness AI, learning a prediction model by minimizing the empirical risk (e.g., cross-entropy) subject to a given fairness constraint has received much attention. To avoid computational difficulty, however, a given fairness constraint is replaced by a surrogate fairness constraint as the 0-1 loss is replaced by a convex surrogate loss for classification problems. In this paper, we investigate the validity of existing surrogate fairness constraints and propose a new surrogate fairness constraint called SLIDE, which is computationally feasible and asymptotically valid in the sense that the learned model satisfies the fairness constraint asymptotically and achieves a fast convergence rate. Numerical experiments confirm that the SLIDE works well for various benchmark datasets.

## 1. Introduction

Recently, AI (Artificial Intelligence) is being used as decision making tools in various domains such as credit scoring, criminal risk assessment, education of college admissions (Angwin, Larson, Mattu and Kirchner (2016)) and sentiment analysis (Mahendhiran and Subramanian (2018)). As AI has a wide range of influences on human social life, issues of transparency and ethics of AI are emerging. However, it is widely known that due to the existence of historical bias in data against ethics or regulatory frameworks for fairness, trained AI models based on such biased data could also impose bias or unfairness against a certain sensitive group (e.g., non-white, women) (Kleinberg, Ludwig, Mullainathan and Rambachan (2018); Mehrabi, Morstatter, Saxena, Lerman and Galstyan (2019)). Therefore, designing an AI algorithm that is accurate and fair simultaneously has become a crucial research topic.

The two important issues in fairness AI are definitions of fairness and algorithms to learn fair prediction models. There are various definitions of fairness AI, which are roughly categorized into two groups - *group fairness* and *individual fairness*. Group fairness (Calders, Kamiran and Pechenizkiy (2009); Barocas and Selbst (2016); Hardt, Price and Srebro (2016)) focuses on treating fairly each sensitive group while individual fairness (Dwork, Hardt, Pitassi,

Reingold and Zemel (2012)) focuses on treating fairly any similar individuals.

Once the definition of fairness is selected, the next step for fairness AI is to choose a learning algorithm to find a fair classifier that is not only accurate but also fair. Most fair learning algorithms belong to one of the three categories - pre-processing, in-processing and post-processing methods.

Pre-processing methods remove bias in training dataset or find a fair representation with respect to sensitive variables before the training phase and learn AI models based on de-biased data or fair representations. Zemel, Wu, Swersky, Pitassi and Dwork (2013) proposes a method to learn fair representations based on a clustering algorithm and uses them as feature vectors for solving downstream tasks fairly. After this work, various pre-processing methods including Feldman, Friedler, Moeller, Scheidegger and Venkatasubramanian (2015); Webster, Recasens, Axelrod and Baldrige (2018); Xu, Yuan, Zhang and Wu (2018); Creager, Madras, Jacobsen, Weis, Swersky, Pitassi and Zemel (2019) have been developed.

In-processing methods generally train an AI model by minimizing the cost function subject to a given fairness constraint. Various fairness constraints have been proposed in Kamishima, Akaho, Asoh and Sakuma (2012); Goh, Cotter, Gupta and Friedlander (2016); Zafar, Valera, Rogniguez and Gummadi (2017); Agarwal, Beygelzimer, Dudik, Langford and Wallach (2018); Cotter, Jiang and Sridharan (2019); Celis, Huang, Keswani and Vishnoi (2019); Zafar, Valera, Gomez-Rodriguez and Gummadi (2019); Cho, Suh and Hwang (2020); Vogel, Bellet and Cl  men  on (2020), to name just a few. In particular, Goh et al. (2016); Wu, Zhang and Wu (2019) and Jiang, Pacchiano, Stepleton, Jiang and Chiappa (2020) use the hinge-surrogate fairness constraint serving as the baseline method in this paper.

Post-processing methods firstly learn an AI model without any fairness constraint and then transform the decision boundary or score function of the trained AI model for each

<sup>\*</sup> This work was supported by Institute for Information & communications Technology Planning & Evaluation(IITP) grant funded by the Korea government(MSIT) (No. 2019-0-01396, Development of framework for analyzing, detecting, mitigating of bias in AI model and training data).

<sup>\*</sup>Corresponding author at: Department of Statistics, Seoul National University, Republic of Korea.

✉ kwkim.online@gmail.com (K. Kim); ilsang.ohn@inha.ac.kr (I. Ohn); sarah58833@gmail.com (S. Kim); ydkim0903@gmail.com (Y. Kim)

ORCID(s):

<sup>1</sup>The work was carried out while being affiliated to the Department of Applied and Computational Mathematics and Statistics, University of Notre Dame, United States of America.

<sup>2</sup>The work was carried out while being affiliated to the Department of Statistics, Seoul National University, Republic of Korea.

sensitive group to satisfy a given fairness constraint. For example, Jiang et al. (2020) proposes to map unfair prediction models to the Wasserstein distance-based barycenter. See Hardt et al. (2016); Kamiran, Karim and Zhang (2012); Fish, Kun and Lelkes (2016); Corbett-Davies, Pierson, Feller, Goel and Huq (2017); Pleiss, Raghavan, Wu, Kleinberg and Weinberger (2017); Chzhen, Denis, Hebiri, Oneto and Pontil (2019); Wei, Ramamurthy and Calmon (2020) for other post-processing methods.

In this paper, we are concerned with in-processing fairness AI algorithms. A difficulty in in-processing algorithms is that most fairness constraints involve the indicator function  $I(\cdot > 0)$  which makes the optimization infeasible. To resolve this problem, a popular approach is to replace  $I(\cdot > 0)$  by a computationally easier surrogate function such as the hinge function  $(1 + \cdot)_+$ . This hinge function is the tight convex upper bound of the indicator function and hence popularly used for a surrogate loss function of the 0-1 loss. Moreover, it is known that the hinge loss is Fisher-consistent in the sense that the minimizer of the population risk with respect to the hinge loss is equal to the Bayes risk (Zhang (2004); Bartlett, Jordan and McAuliffe (2006); Blanchard, Bousquet and Massart (2008)). Thus, we can estimate the Bayes classifier consistently by minimizing the empirical risk with respect to the hinge loss under regularity conditions.

The question we address in this paper is whether this nice property of the hinge function as a surrogate loss of the 0-1 loss is still valid for the fairness constraint. That is, we investigate whether in-processing learning algorithms with a surrogate fairness constraint yield prediction models which are (asymptotically) fair in terms of the original fairness constraint. Asymptotic properties of fairness AI algorithms have been studied by Woodworth, Gunasekar, Ohannessian and Srebro (2017) and Donini, Oneto, Ben-David, Shawe-Taylor and Pontil (2018). Woodworth et al. (2017) proposed a two-step procedure to find a prediction model which is asymptotically fair. However, as noted by the authors, the proposed algorithm is not computationally feasible since it involves indicator functions in the objective function to be minimized. Hence, in practice, the indicator function in constraint should be replaced by a surrogate function.

For representative studies of using surrogate fairness constraint functions, the hinge-surrogate (Goh et al. (2016); Wu et al. (2019); Jiang et al. (2020)) and the linear-surrogate (Donini et al. (2018); Yurochkin and Sun (2020); Chuang and Mroueh (2021)) are popularly used. However, no theoretical results about the validity of such surrogate fairness constraints have been studied. Moreover, Lohaus, Perrot and Luxburg (2020) raises an issue that using such existing surrogate fairness constraints cannot guarantee a given fairness constraint due to the gap between the original constrained function space and the surrogate one. We also provide Figure 2, which illustrates that the hinge-surrogate fairness constraint used in Goh et al. (2016); Wu et al. (2019); Jiang et al. (2020) does not provide the optimal model under the original fairness constraint.

We take those fairness surrogate constraints as state-of-the-art baselines in our numerical experiments. We refer to the later section of experiments (Section 5) for precise descriptions of baseline methods. In summary, a proper surrogate function is highly required for learning fair models.

The aim of this research is to propose a new surrogate fairness constraint that makes the optimization feasible and provides the optimal prediction model under the original fairness constraint asymptotically. For this purpose, we develop a new surrogate function called SLIDE for the indicator function. We prove that the minimizer of the empirical risk subject to the SLIDE-surrogate fairness constraint is asymptotically equivalent to the minimizer of the population risk under the original fairness constraint.

Our contributions are summarized as follows.

- We propose a new surrogate fairness constraint called SLIDE, which is computationally feasible and has desirable theoretical properties.
- We prove that the SLIDE is an asymptotically valid surrogate fairness constraint by deriving the fairness convergence rate as well as the risk convergence rate of prediction models trained by in-processing methods with the SLIDE-surrogate fairness constraint.
- We empirically demonstrate by analyzing several benchmark datasets that the SLIDE-surrogate fairness constraints are superior to or never worse than the existing surrogate fairness constraints.

## 2. Learning algorithms for fairness AI: Review

Let  $(Y, \mathbf{X}, Z)$  be the random vector of a triplet of output, input and sensitive variables, whose distribution is  $P$ . For simplicity, we consider a binary classification problem (i.e.  $Y \in \{-1, 1\}$ ) and a binary sensitive variable (i.e.  $Z \in \{0, 1\}$ ). For a given loss function  $l$  and a class of prediction models  $\mathcal{F}$ , the aim of supervised learning is to find  $f^*$  defined as  $f^* = \operatorname{argmin}_{f \in \mathcal{F}} \mathbf{E}(l(Y, f(\mathbf{X})))$ . Due to historical biases or social prejudices, the optimal prediction model  $f^*$  would not be socially acceptable because it treats certain groups or individuals unfairly. Thus, we want to search  $f$  which is fair and at the same time makes the population risk  $\mathbf{E}(l(Y, f(\mathbf{X})))$  as small as possible.

Suppose that  $\mathcal{F}_{\text{fair}}$  is a subset of  $\mathcal{F}$  which consists of all fair prediction models. Then, the goal of fair supervised learning is to find  $f_{\text{fair}}^*$  defined as

$$f_{\text{fair}}^* = \operatorname{argmin}_{f \in \mathcal{F}_{\text{fair}}} \mathbf{E}(l(Y, f(\mathbf{X}))).$$

There exist numerous definitions for the fairness model class  $\mathcal{F}_{\text{fair}}$ , most of which can be formulated as

$$\mathcal{F}_{\text{fair}} = \{f \in \mathcal{F} : \phi(f) \leq \alpha\} \quad (1)$$

for a positive constant  $\alpha$ , where  $\phi : \mathcal{F} \rightarrow [0, \infty)$  is a so called *fairness constraint function* corresponding to

a given definition of fairness. In the next subsection, two representative fairness constraints are explained, which we focus for theoretical derivations and empirical studies. Our theoretical results, however, can be applied to most of other fairness constraints without much modification.

### 2.1. Examples of fairness constraints

We consider two representative fairness constraints - one for group fairness and the other for individual fairness. For a given real-valued function  $f$  and an input  $\mathbf{X}$ , the corresponding classifier is constructed by  $\text{sign}\{f(\mathbf{X})\}$ .

**Disparate Impact:** The first fairness constraint is disparate impact (DI) (Barocas and Selbst (2016)). A prediction model  $f$  satisfies the  $\alpha$ -DI if  $\phi(f) \leq \alpha$ , where

$$\phi(f) = |\mathbf{P}(f(\mathbf{X}) \geq 0 | Z = 0) - \mathbf{P}(f(\mathbf{X}) \geq 0 | Z = 1)|. \quad (2)$$

Other group fairness constraints can be defined by replacing  $\mathbf{P}(f(\mathbf{X}) \geq 0 | Z = z)$  in (2) for  $z \in \{0, 1\}$  by other conditional probabilities. For example, the equalized odds (EO) and equal opportunity (EqOpp) from Hardt et al. (2016) are defined by replacing  $\mathbf{P}(f(\mathbf{X}) \geq 0 | Z = z)$  into  $\mathbf{P}(f(\mathbf{X}) \geq 0 | Z = z, Y = y)$  for  $y \in \{-1, 1\}$  and  $\mathbf{P}(f(\mathbf{X}) \geq 0 | Z = z, Y = 1)$  respectively.

**Uniform Individual Fairness:** Individual fairness requires that similar individuals should be treated similarly. Dwork et al. (2012) introduces the initial notion of individual fairness: we say a classifier  $f \in \mathcal{F}$  is individually fair if it satisfies the Lipschitz property, i.e., for every  $\mathbf{x}, \mathbf{x}' \in \mathcal{X}$ ,  $D(f(\mathbf{x}), f(\mathbf{x}')) \leq d(\mathbf{x}, \mathbf{x}')$  with respect to a similarity metric  $D(\cdot, \cdot)$  between prediction models and a similarity metric  $d(\cdot, \cdot)$  between individuals. Yona and Rothblum (2018) introduces a relaxed notion: a classifier  $f \in \mathcal{F}$  is  $(\alpha, \gamma)$ -approximately individually fair if it satisfies  $\mathbf{P}_{\mathbf{x}, \mathbf{x}'}(D(f(\mathbf{x}), f(\mathbf{x}')) - d(\mathbf{x}, \mathbf{x}') > \gamma) \leq \alpha$  for a given  $\gamma > 0$ . In this paper, we consider a new definition of individual fairness called  $(\alpha, \gamma, \epsilon)$ -uniform individual fair (UIF) defined as  $\phi(f; \gamma, \epsilon) \leq \alpha$ , where

$$\phi(f; \gamma, \epsilon) := \mathbf{P}\left(\sup_{\mathbf{v}: d(\mathbf{X}, \mathbf{v}) \leq \epsilon} D(f(\mathbf{X}), f(\mathbf{v})) > \gamma\right). \quad (3)$$

The definition of UIF is motivated by the definition of SenSel from Yurochkin and Sun (2020) which requires that

$$\mathbf{E}\left(\sup_{\mathbf{v}: d(\mathbf{X}, \mathbf{v}) \leq \epsilon} D(f(\mathbf{X}), f(\mathbf{v}))\right) \leq \alpha.$$

We replace the expectation by the probability even though one more parameter (i.e.  $\gamma$ ) is needed. In Section 5, we show that UIF is better than SenSel.

### 2.2. Learning algorithms for fairness AI

Let  $(y_1, \mathbf{x}_1, z_1), \dots, (y_n, \mathbf{x}_n, z_n)$  be given training dataset which are assumed to be independent realizations of  $(Y, \mathbf{X}, Z)$ . Let  $\phi_n$  be the empirical version of  $\phi$ . The  $\phi_n$  for DI and UIF are given as

$$\phi_n(f) = \left| \frac{1}{n_0} \sum_{i: z_i=0} \mathbf{I}(f(\mathbf{x}_i) > 0) - \frac{1}{n_1} \sum_{i: z_i=1} \mathbf{I}(f(\mathbf{x}_i) > 0) \right|$$

(4)

and

$$\phi_n(f; \gamma, \epsilon) = \frac{1}{n} \sum_{i=1}^n \mathbf{I}(D(f(\mathbf{x}_i), f(\mathbf{v}'_i)) > \gamma) \quad (5)$$

respectively, where  $n_z = \sum_{i=1}^n \mathbf{I}(z_i = z)$  and  $\mathbf{v}'_i = \arg \max_{\mathbf{v}: d(\mathbf{x}_i, \mathbf{v}) \leq \epsilon} D(f(\mathbf{x}_i), f(\mathbf{v}))$ .

Let  $\mathcal{F}_{n, \alpha} = \{f \in \mathcal{F} : \phi_n(f) \leq \alpha\}$ . Most in-processing fair learning algorithms try to minimize the empirical risk  $L_n(f)$  on  $\mathcal{F}_{n, \alpha}$ , where  $L_n(f) = \sum_{i=1}^n l(y_i, f(\mathbf{x}_i))/n$ . However, this optimization is hard since  $\phi_n$  is not continuous. Typically this problem is resolved by use of a surrogate fairness constraint. One of the most popular surrogate fairness constraint is to replace the indicator function  $\mathbf{I}(\cdot \geq 0)$  in  $\phi_n$  by the hinge function  $(1 + \cdot)_+$ , which we denote  $\phi_n^{\text{hinge}}(f)$  and  $\phi_n^{\text{hinge}}(f; \gamma, \epsilon)$ . Then, we learn a prediction model by minimizing the empirical risk subject to  $\phi_n^{\text{hinge}}(f) \leq \alpha$  which is similar to Goh et al. (2016); Wu et al. (2019) and Jiang et al. (2020). We note that not only for the hinge-surrogate constraint, but one can also consider other existing surrogate constraints that are used in Zafar et al. (2017); Donini et al. (2018); Madras, Creager, Pitassi and Zemel (2018) and Chuang and Mroueh (2021).

## 3. SLIDE: A new surrogate fairness constraint

For a fixed  $\alpha > 0$  and any  $\delta > 0$ , we say that a trained prediction model  $\hat{f}_n$  is fairness-consistent if  $\mathbf{P}\{\phi(\hat{f}_n) \leq \alpha + \delta\} \rightarrow 1$  as  $n \rightarrow \infty$ . The aim of this section is to propose a new surrogate fairness constraint with which the corresponding (in-processing) trained prediction model is fairness-consistent.

The hinge function is popularly used as a surrogate loss function of the 0-1 loss in classification problems, and it is shown that the resulting estimator is risk-consistent in the sense that the mis-classification error of the trained prediction models converges to that of the Bayes classifier (Zhang (2004); Bartlett et al. (2006); Blanchard et al. (2008)). This nice property of the hinge function, however, would not hold for fairness-consistency. This is mainly because the surrogate fairness constraint may not be asymptotically equivalent to the original fairness constraint. To resolve this problem, we propose a new surrogate function so-called SLIDE for the indicator function  $\mathbf{I}(\cdot > 0)$  such that the corresponding surrogate fairness constraint is asymptotically equivalent to the original fairness constraint, and thus the resulting prediction model becomes fairness-consistent as well as risk-consistent.

### 3.1. Proposed surrogate fairness constraint:

#### SLIDE

For a given  $\tau > 0$ , the SLIDE function  $v_\tau(\cdot) : \mathbb{R} \rightarrow [0, 1]$  is defined as

$$v_\tau(z) = \frac{z}{\tau} \mathbf{I}(0 < z \leq \tau) + \mathbf{I}(z > \tau). \quad (6)$$

Figure 1 compares the 0-1, the hinge and SLIDE functions. The function  $v_\tau$  looks similar to a slide so that we call it SLIDE. Note that the SLIDE function is a lower bound of the 0-1 function while the hinge function is an upper bound. In addition, the SLIDE function is non-convex while the hinge function is convex. The non-convexity would make the corresponding optimization more difficult, but our experiments suggest that standard gradient descent based optimization algorithms work well with the SLIDE function. Moreover, it is possible to apply convex-concave procedure (CCCP) of Yuille and Rangarajan (2002) since  $v_\tau(\cdot)$  is decomposed by the sum of convex and concave functions. See sections of experiments (Section 5 and E) for details. The empirical SLIDE-surrogate fairness constraints for DI and UIF are obtained by replacing  $I(\cdot > 0)$  in  $\phi_n$  by  $v_\tau(\cdot)$ , which we denote  $\phi_{n,\tau}^{\text{slide}}(f)$  and  $\phi_{n,\tau}^{\text{slide}}(f; \gamma, \epsilon)$ , respectively. We also denote  $\phi_\tau^{\text{slide}}(f)$  and  $\phi_\tau^{\text{slide}}(f; \gamma, \epsilon)$  as population version of both, respectively. For notational simplicity, we omit the superscript ‘‘slide’’ when the meaning is clear.

The SLIDE function is motivated by the  $\Psi$  learning of Shen, Tseng, Zhang and Wong (2003), where  $\Psi(z) = (z/\tau) \cdot I(-\tau < z \leq 0) + I(z > 0)$  is used as a surrogate loss of the negative 0-1 loss. Even though the  $\Psi$  function is an upper bound of the indicator function, it would not be appropriate for a surrogate fairness constraint since  $\phi_n(f)$  depends on samples with  $-\tau < f(\mathbf{x}_i) < 0$  for some  $i \in \{1, \dots, n\}$ . We modify the  $\Psi$  function to have the SLIDE function.

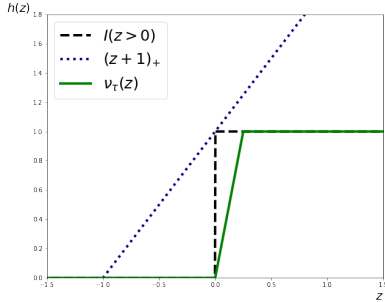


**Figure 1:** Comparison of the 0-1, hinge and SLIDE ( $\tau = 0.25$ ) functions (black long dotted line: the 0-1, blue short dotted line: the hinge, and green solid line: the SLIDE).

### 3.2. Comparison of the SLIDE- and hinge-surrogate fairness constraints with a toy example

Let  $\mathcal{F}_{n,\alpha}^{\text{hinge}} = \{f \in \mathcal{F} : \phi_n^{\text{hinge}}(f) \leq \alpha\}$  and  $\mathcal{F}_{n,\alpha,\tau}^{\text{slide}} = \{f \in \mathcal{F} : \phi_{n,\tau}^{\text{slide}}(f) \leq \alpha\}$ . In this section, by analyzing a toy example, we illustrate that  $\mathcal{F}_{n,\alpha,\tau}^{\text{slide}}$  is closer to the original constraint class  $\mathcal{F}_{n,\alpha}$  than  $\mathcal{F}_{n,\alpha}^{\text{hinge}}$  is.

The left panel of Figure 2 presents the toy dataset with two dimensional samples which are generated from a mixture of two Gaussian distributions whose details are given in Appendix. We consider linear model as  $\mathcal{F} = \{f_\beta(\mathbf{x}) = \beta_1 x_1 + \beta_2 x_2 : \beta := (\beta_1, \beta_2)^\top \in (-2, 2)^2\}$ . For the fairness constraint, we consider the relaxed individual

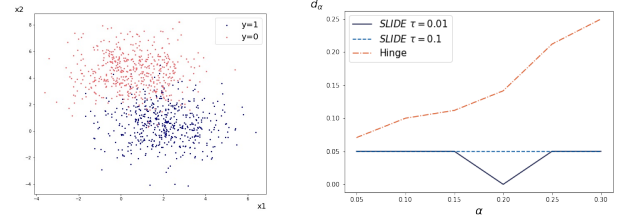


**Figure 2:** (Left) The scatter plot of the 2-D toy dataset (2-component Gaussian Mixture). (Right) Plot of  $\alpha$  vs.  $d_\alpha^{\text{hinge}}$  and  $d_\alpha^{\text{slide}}$  for  $\tau \in \{0.01, 0.1\}$ .

fairness in Yona and Rothblum (2018) as  $\phi_{\text{if}}(f; \gamma) = \mathbf{P}_{\mathbf{X}, \mathbf{X}'} \{D(f(\mathbf{X}), f(\mathbf{X}')) - d(\mathbf{X}, \mathbf{X}') > \gamma\}$  with  $\gamma = 0.3$ , where  $\mathbf{X}'$  is a independent copy of  $\mathbf{X}$ .

We calculate  $\mathcal{F}_{n,\alpha}$ ,  $\mathcal{F}_{n,\alpha,\tau}^{\text{hinge}}$  and  $\mathcal{F}_{n,\alpha,\tau}^{\text{slide}}$  by a grid search and compare them as follows. Let  $\Theta_{n,\alpha} = \{\beta : f_\beta \in \mathcal{F}_{n,\alpha}\}$ , and  $\Theta_{n,\alpha}^{\text{hinge}}$  and  $\Theta_{n,\alpha,\tau}^{\text{slide}}$  are defined accordingly. We obtain those sets of fair parameters by calculating the population version of the fairness constraint values (i.e.,  $\phi_{\text{if}}(f; \gamma)$ ) based on Monte-Carlo simulation at the selected parameters on grids (i.e.,  $(\beta_1, \beta_2)$  on the  $200 \times 200$  grids of  $(-2, 2) \times (-2, 2)$ ).

Let  $D_H(\cdot, \cdot)$  be the Hausdorff distance between two subsets in  $(-2, 2)^2$ . It turns out that

$$D_H(\Theta, \Theta') = \max(D_{H,1}, D_{H,2})$$

where  $D_{H,1} := \sup_{\theta \in \Theta} \inf_{\theta' \in \Theta'} \|\theta - \theta'\|_2$  and  $D_{H,2} := \sup_{\theta' \in \Theta'} \inf_{\theta \in \Theta} \|\theta' - \theta\|_2$  for two subsets  $\Theta$  and  $\Theta'$ . We calculate  $d_\alpha^{\text{hinge}} = \min_{\alpha'} D_H(\Theta_{n,\alpha}, \Theta_{n,\alpha'}^{\text{hinge}})$  and  $d_\alpha^{\text{slide}} = \min_{\alpha'} D_H(\Theta_{n,\alpha}, \Theta_{n,\alpha',\tau}^{\text{slide}})$  for each  $\alpha$ . Then we draw the plot of  $\alpha$  versus  $d_\alpha^{\text{hinge}}$  and  $d_\alpha^{\text{slide}}$  with  $\tau \in \{0.01, 0.1\}$  which is given in the right panel of Figure 2. We consider  $\alpha$  less than 0.3 since the level of fairness for the optimal classifier is around 0.3. Note that  $d_\alpha^{\text{hinge}}$  is getting larger as  $\alpha$  increases while  $d_\alpha^{\text{slide}}$  stays at a lower level regardless of  $\alpha$ . That is, the hinge-surrogate fairness constraint does not approximate the original fairness constraint well and thus the corresponding fair prediction model would be suboptimal. In contrast, the SLIDE-surrogate fairness constraint approximates the original fairness constraint relatively well. This phenomenon is still observed for the two-moon dataset and for DI, whose results are given in Appendix E.

## 4. Theoretical analysis

In this section, we consider the estimated prediction model  $\hat{f}_n$  obtained by minimizing the empirical risk  $L_n(f)$  on  $\mathcal{F}_{n,\alpha+\delta_n,\tau_n}^{\text{slide}} = \{f \in \mathcal{F} : \phi_{n,\tau_n}^{\text{slide}}(f) \leq \alpha + \delta_n\}$  for given  $\tau_n$  and  $\delta_n$  converging to 0, and study asymptotic properties of  $\hat{f}_n$ . In particular, we derive the upper bound of  $\tau_n$  such that the fair prediction model with the SLIDE-surrogate fairness constraint is asymptotically equivalent to the fair prediction model with the original fairness constraint. Note that a larger  $\tau_n$  is better in view of computation since the

**Table 1**

A list of mathematical notations and symbols.

Notation (Reference if exists)	Description
$\mathbf{X} \in \mathbb{R}^d$ $Y \in \{-1, 1\}$ $Z \in \{0, 1\}$	Input random vector Output random variable Sensitive random variable
$f$ $\hat{f}_n$ $f_\alpha^*$	A prediction model The fair model learned by the SLIDE-surrogate fairness constraint The true fair model
$\phi$ (Equations (2), (3)) $\phi_\tau^{\text{slide}}$ $\phi_\tau^{\text{hinge}}$ $\alpha$ (Equation (1)) $\gamma$ (Equation (3)) $\epsilon$ (Equation (3))	A fairness constraint function The SLIDE-surrogate constraint function for a given $\phi$ The hinge-surrogate constraint function for a given $\phi$ Upper bound of constraint function, i.e., level of fairness The relaxation parameter for UIF The maximum perturbation norm for UIF
$v_\tau$ (Equation (6))	The SLIDE function with $\tau > 0$

SLIDE function becomes less non-convex. For the sake of readers' convenient, we list the mathematical notations and symbols introduced in the previous sections in Table 1.

For a given estimator  $\hat{f}_n$ , we say that the fairness convergence rate of  $\hat{f}_n$  is  $a_n$  if  $\phi(\hat{f}_n) \leq \alpha + a_n$  in probability. Similarly, we say that the  $l$ -excess risk convergence rate of  $\hat{f}_n$  is  $b_n$  if  $\mathcal{E}_l(\hat{f}_n, f_\alpha^*) := \mathbf{E}(l(Y, \hat{f}_n(\mathbf{X}))) - \mathbf{E}(l(Y, f_\alpha^*(\mathbf{X}))) \leq b_n$  in probability, where  $f_\alpha^*$  is the true minimizer of  $\mathbf{E}(l(Y, f(\mathbf{X})))$  among all measurable functions  $f$  with  $\phi(f) \leq \alpha$ . We derive  $a_n$  and  $b_n$  in terms of  $\tau_n$  and  $\delta_n$  as well as the complexity of  $\mathcal{F}$ , that provide a guide to choose  $\tau_n$  and  $\delta_n$ . We allow the class of models  $\mathcal{F}$  to depend on the sample size, denoted by  $\mathcal{F}_n$ , which is popularly used in nonparametric regression contexts to avoid overfitting. For notational simplicity, we drop the subscript  $n$  whenever the meaning is clear.

For technical reasons, we derive the fairness and  $l$ -excess convergence rates of  $\hat{f}_n$  which depend on  $\hat{f}_n$  itself. To be more specific, we assume that there exists a constant  $M_f > 0$  depending on  $f \in \mathcal{F}$  such that

$$|\phi(f) - \phi_{\tau_n}^{\text{slide}}(f)| \leq M_f \tau_n.$$

For example of UIF, we can set  $M_f = \sup_{r \in [-v, v]} g_D(r)$ , where  $g_D$  is the density of  $\sup_{\mathbf{v}: d(\mathbf{X}, \mathbf{v}) \leq \epsilon} D(f(\mathbf{X}), f(\mathbf{v}))$  and  $v$  is a positive constant greater than  $\tau_n$ . Our convergence rates depend on  $M_{\hat{f}_n}$  as well as  $\tau_n$ .

#### 4.1. Fairness convergence rate

The fairness convergence rate depends on the two quantities: (1) the complexity of  $\mathcal{F}$  and (2) the choice of  $\tau_n$  and  $\delta_n$ . For the complexity of  $\mathcal{F}$ , the empirical Rademacher complexity defined as

$$\hat{\mathcal{R}}(\mathcal{F}) = \frac{1}{n} \mathbf{E}_{\sigma_i \sim U(\{\pm 1\})^n} \left( \sup_{f \in \mathcal{F}} \sum_{i=1}^n \sigma_i f(\mathbf{X}_i) \right)$$

is a standard measure. The following two theorems show that how the fairness convergence rates depend on  $\tau_n$  and  $\delta_n$  as well as the empirical Rademacher complexity.

**Theorem 1** (Fairness convergence rate for DI). *When  $\phi$  is DI, the fairness convergence rate of  $\hat{f}_n$  is given by*

$$a_n = \mathcal{O} \left( \delta_n + M_{\hat{f}_n} \tau_n + \sum_{z \in \{0, 1\}} \hat{\mathcal{R}}_z(v_{\tau_n}(\mathcal{F})) + \sqrt{\frac{\log n}{n}} \right),$$

where  $v_{\tau_n}(\mathcal{F}) := \{v_{\tau_n}(f) : f \in \mathcal{F}\}$ .

**Theorem 2** (Fairness convergence rate for UIF). *When  $\phi$  is UIF with the parameters  $\gamma$  and  $\epsilon$ , the fairness convergence rate of  $\hat{f}_n$  is given by*

$$a_n = \mathcal{O} \left( \delta_n + M_{\hat{f}_n} \tau_n + \hat{\mathcal{R}}(v_{\tau_n} \circ \eta(\mathcal{F})) + \sqrt{\frac{\log n}{n}} \right),$$

where  $v_{\tau_n} \circ \eta(\mathcal{F}) = \{v_{\tau_n} \circ \eta_f : f \in \mathcal{F}\}$  and  $\eta_f(\mathbf{x}) := D(f(\mathbf{x}), f(\mathbf{x}')) - \gamma$ .

Note that the fairness convergence rates in Theorems 1 and 2 cannot be faster by  $\sqrt{\log n/n}$ . Theorems 1 and 2 imply that the largest  $\tau_n$  without sacrificing the fairness convergence rate is  $\mathcal{O}(\sqrt{\log n/n})$ . A situation is similar for  $\delta_n$  in the sense that  $\delta_n = \mathcal{O}(\sqrt{\log n/n})$  makes the constrained function space  $\mathcal{F}_{n, \alpha + \delta_n, \tau_n}^{\text{slide}}$  be as large as possible without affecting the fairness convergence rate. If the Rademacher complexities are larger than  $\mathcal{O}(\sqrt{\log n/n})$ , we can let  $\tau_n$  and  $\delta_n$  be even larger.

Desirable upper bounds of the Rademacher complexities could not be derived directly from that of  $\mathcal{F}$  since the Lipschitz constant of the SLIDE function  $v_{\tau_n}$  diverges as  $n \rightarrow \infty$ . We calculate the upper bounds of the Rademacher complexities by calculating the metric entropy of  $v_\tau \circ \eta(\mathcal{F})$  directly. The results for the case of  $\mathcal{F}$  being linear model class are provided in Appendix. For deep neural networks, we consider a case where the class  $\mathcal{F}$  of prediction models depends on the sample size  $n$  and calculate empirical Rademacher complexities to derive ( $l$ -excess) risk convergence rates in the following subsection.

## 4.2. Risk convergence rate

The convergence rate of the ( $l$ -excess) risk depends on various choices including the loss function and the model class  $\mathcal{F}$ . We use the logistic loss  $l(y, f) = \log(1 + \exp(-yf))$ . For  $\mathcal{F}$ , we consider deep neural networks with the ReLU activation,  $L_n$  many layers,  $N_n$  many nodes at each layer,  $S_n$  many non-zero weights and biases that are bounded by  $B_n$ , the final output value being bounded by  $F_n$ . To derive the risk convergence rate, we assume that  $f_\alpha^*$  belongs to the Hölder space with smoothness  $\zeta$  (see the definition of Hölder space in Appendix). The next theorem derives the risk convergence rates for DI and UIF as well as the fairness convergence rates.

**Theorem 3** (Risk convergence rates for DI and UIF). *Suppose that  $n_1/n_0 \rightarrow s \in (0, \infty)$  and that  $\phi(f)$  is  $M$ -Lipschitz with respect to  $\|\cdot\|_\infty$ . That is,  $|\phi(f_1) - \phi(f_2)| \leq M\|f_1 - f_2\|_\infty$  for some constant  $M > 0$ . Let  $b_n := n^{-\frac{\zeta}{2\zeta+d}}(\log n)^{3/2}$ . Moreover, assume that  $\delta_n/b_n \rightarrow \infty$  as  $n \rightarrow \infty$ . Then, for both DI and UIF, there exist positive sequences  $L_n, N_n, S_n, B_n$  and  $F_n$  such that*

$$\begin{aligned} \mathcal{E}(\hat{f}_n, f_\alpha^*) &\leq \mathcal{O}(b_n + M_{\hat{f}_n} \tau_n) \\ \phi(\hat{f}_n) &\leq \alpha + \mathcal{O}(\delta_n + b_n + M_{\hat{f}_n} \tau_n) \end{aligned}$$

with probability at least  $1 - 1/n$ .

Assume that  $M_{\hat{f}_n}$  is bounded. The largest rate of  $\tau_n$  that minimizes the risk convergence rate and fairness convergence rate simultaneously is  $b_n$  (i.e.,  $\tau_n = \mathcal{O}(b_n)$ ), which makes the two convergence rates be almost equal provided  $\delta_n/b_n$  diverges slowly (e.g.,  $\log n$  order). This result implies that we can set  $\tau_n$  larger when  $\mathcal{F}$  is more complex (i.e.,  $\zeta$  is smaller and hence  $b_n$  is larger) and vice versa.

For standard classification problems, the risk convergence rate could be faster than  $1/\sqrt{n}$  and hence the risk convergence rate in Theorem 3 looks suboptimal. However, this slower convergence rate is unavoidable since  $f_\alpha^*$  is not the global minimizer of the population risk  $\mathbf{E}\{l(Y, f(\mathbf{X}))\}$  among all measurable functions. We believe that the risk convergence rate in Theorem 3 would be optimal. Here, we note that Table 1 in Appendix summarizes mathematical notations used in this section.

## 4.3. Remarks on $M_{\hat{f}_n}$

The convergence rates in Theorems 1, 2 and 3 would be meaningful only if  $M_{\hat{f}_n}$  is not too large (i.e., bounded). Let  $\tau_n = \mathcal{O}(b_n)$ , which is the largest  $\tau_n$  that does not change the convergence rates. In Proposition 1 of Appendix, we prove that  $M_{\hat{f}_n} \leq M_{n, \hat{f}_n} + \mathcal{O}(1)$ , where

$$M_{n, f} = |\phi_{n, -\tau_n}^{\text{slide}}(f; \gamma, \epsilon) - \phi_{n, \tau_n}^{\text{slide}}(f; \gamma, \epsilon)|/\tau_n$$

for UIF, where  $\phi_{n, -\tau_n}^{\text{slide}}$  is the opposite SLIDE-surrogate fairness constraint (i.e.,  $v_\tau$  in  $\phi_{n, \tau_n}^{\text{slide}}$  is replaced by  $v_{-\tau} = \frac{z}{\tau} \mathbf{I}(-\tau < z \leq 0) + \mathbf{I}(z > 0)$ ). The population version of  $\phi_{-\tau_n}^{\text{slide}}$  can be defined similarly. A formula of  $M_{n, f}$  for DI is

provided in Proposition 2 of Appendix. Thus, when  $M_{n, \hat{f}_n}$  is not large, we expect that  $M_{\hat{f}_n}$  is also small.

The above result provides a way of using the SLIDE-surrogate fairness constraint in practice. First, we learn  $f$  by  $\hat{f}_n$  with the SLIDE-surrogate fairness constraint. Then, if  $M_{n, \hat{f}_n}$  is not too large, we keep using  $\hat{f}_n$  for prediction. Otherwise, we abort  $\hat{f}_n$  and resort to other fairness AI algorithms. For example, we decide that  $M_{n, \hat{f}_n}$  is too large if  $M_{n, \hat{f}_n} \tau_n$  is larger than 10% of  $\phi(\hat{f}_n)$ . In Table 7 in Appendix E, we observe that  $M_{n, \hat{f}_n} \tau_n$  is not larger than 10% of  $\phi(\hat{f}_n)$  for the datasets analyzed in our numerical studies, which amply supports the validity of the SLIDE-surrogate fairness constraints.

## 5. Experiments

We compare the SLIDE-surrogate fairness constraint to the hinge-surrogate fairness constraint by analyzing three benchmark datasets for both group fairness and individual fairness. For the class of models, we use single hidden layer deep neural networks. Details about learning algorithms are described in Appendix.

**Datasets** We analyze three public datasets popularly used in fairness AI: (1) *Adult* dataset from Dua and Graff (2017), (2) *Bank* dataset from Lichman (2013), and (3) *Law* dataset from SEAPHE<sup>1</sup>. They have gender, age and race as the sensitive variable, respectively. For each dataset, we split the whole dataset into training, validation and test datasets with ratio 60% : 20% : 20% randomly and repeat this random splitting three times.

**Performance measures** For prediction accuracy, we use two measures: accuracy (Acc) and balanced accuracy (BA). The balanced accuracy, which is considered by Yurochkin, Bower and Sun (2020); Yurochkin and Sun (2020), is an average of the accuracies in each class of label  $y = -1$  and  $y = 1$ . For assessing fairness, we calculate DI on test data for group fairness. For individual fairness, we use the consistency (Con.) of prediction considered by Yurochkin et al. (2020); Yurochkin and Sun (2020). Con. measures how frequently the predictive class labels of two inputs that are the same except the sensitive variable coincide. Note that a larger value of Con. means that the prediction model is more individually fair.

**Optimization algorithms** To learn a fair prediction model, we minimize  $L_n(f) + \lambda \phi_n(f)$  on  $f \in \mathcal{F}$  for a given surrogate fairness constraint  $\phi_n$ , where  $\lambda$  is the Lagrangian multiplier. For  $\lambda$ , we fix the accuracy at a certain level and choose  $\lambda$  such that such that the accuracy of  $\hat{f}_{n, \lambda}$ , a (local) minimizer of  $L_n(f) + \lambda \phi_n(f)$ , on the validation data is closest to the fixed accuracy. Then, we compare the level of fairness. Since deep neural networks and the SLIDE function are highly non-linear, we train multiple models with multiple random

<sup>1</sup><http://www.seaphe.org/databases.php>

initial parameters and then select the most fair model. We use the Adam optimizer of Kingma and Ba (2015) for the optimization.

For the SLIDE-surrogate, we try another optimization algorithm where the solutions obtained with the hinge-surrogate fairness constraint are used as initial solutions, which we call the hybrid SLIDE (HySLIDE) algorithm. By comparing the SLIDE (a gradient descent algorithm with random initials) and the HySLIDE, we can investigate how sensitive the SLIDE-surrogate fairness constraint is to the choice of initials. In addition, we apply the CCCP algorithm of Yuille and Rangarajan (2002) to the SLIDE + UIF, whose details and results are provided in Appendix.

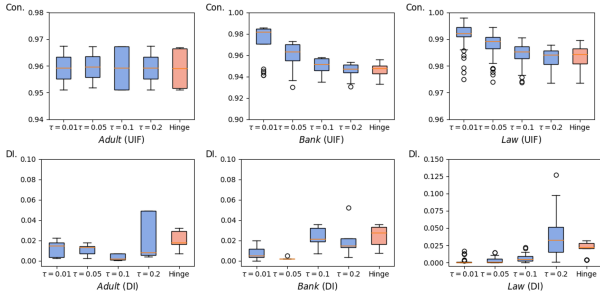


**Figure 3:** Box plots of levels of fairness (upper - Con., lower - DI) of fair models learned by the SLIDE-surrogate constraint with  $\tau \in \{0.01, 0.05, 0.1, 0.2\}$  and the hinge-surrogate constraint on *Adult*, *Bank*, and *Law* test datasets.

Figure 3 draws the box plots of the levels of fairness of the fair prediction models learned with the SLIDE-surrogate and hinge-surrogate fairness constraints. The implication of Figure 3 is that performance of the SLIDE does not strongly depend on the value of  $\tau$  as long as  $\tau$  lies in a reasonable range (i.e., (0.01, 0.2)).

The SLIDE-surrogate fairness constraint has one more regularization parameter  $\tau$  compared to the hinge-surrogate fairness constraint. To make the comparison fair, we select  $\tau$  randomly from (0.01, 0.2) along with a random initial solution. For the hinge-surrogate fairness constraint, we learn multiple prediction models corresponding to multiple random initial parameters and choose the most fair model among those whose accuracies on the validation dataset are similar to a priori given accuracy. Similarly, for the SLIDE-surrogate fairness constraint, we learn multiple prediction models corresponding to multiple pairs of randomly selected  $\tau$  and randomly selected initial parameters and choose the most fair model.

### 5.1. Group fairness

We compare the SLIDE-surrogate and hinge-surrogate fairness constraints for DI. Table 2 summarizes the results, which indicate that the SLIDE-surrogate fairness constraint performs better than the hinge-surrogate fairness constraint for DI. In addition, it is noticeable that the SLIDE outperforms the HySLIDE.

Furthermore, we compare the SLIDE-surrogate fairness constraint with other state-of-the-art methods, Zafar et al.

**Table 2**

Group fairness (DI) performances (Acc(%), BA(%), DI) of fair models learned by the SLIDE-surrogate and the hinge-surrogate constraints on *Adult*, *Bank* and *Law* test datasets.

Dataset	Method	Acc	BA	DI
<i>Adult</i>	DI + Hinge	82.80	72.34	.013 (.001)
	DI + SLIDE	82.19	72.14	<b>.007</b> (.003)
	DI + HySLIDE	82.24	72.33	.010 (.002)
<i>Bank</i>	DI + Hinge	90.07	73.33	.015 (.002)
	DI + SLIDE	90.24	73.22	<b>.013</b> (.002)
	DI + HySLIDE	90.01	73.42	.016 (.003)
<i>Law</i>	DI + Hinge	82.51	59.24	.013 (.004)
	DI + SLIDE	82.49	58.99	<b>.008</b> (.003)
	DI + HySLIDE	82.41	59.54	.014 (.003)

**Table 3**

Group fairness (DI) performances (Acc(%), BA(%), DI) of fair models learned by the state-of-the-art baseline methods (DI + Cov from Zafar et al. (2017) and DI + Linear from Donini et al. (2018)) on *Adult*, *Bank* and *Law* test datasets.

Dataset	Method	Acc	BA	DI
<i>Adult</i>	DI + Cov	82.11	72.50	.018 (.003)
	DI + Linear	82.09	72.05	.016 (.003)
	DI + SLIDE	82.19	72.14	<b>.007</b> (.003)
<i>Bank</i>	DI + Cov	90.04	73.41	.029 (.004)
	DI + Linear	89.35	73.35	.016 (.002)
	DI + SLIDE	90.24	73.22	<b>.013</b> (.002)
<i>Law</i>	DI + Cov	82.50	58.95	.020 (.003)
	DI + Linear	82.40	58.83	.014 (.001)
	DI + SLIDE	82.49	58.99	<b>.008</b> (.003)

(2017) and Donini et al. (2018) in Table 3. Zafar et al. (2017) used a covariance-surrogate constraint for DI (DI + Cov), and Donini et al. (2018) used a linear-surrogate constraint for equalized odds so that we simply modified it to DI (DI + Linear). In Table 3, the SLIDE-surrogate fairness constraint outperforms the other state-of-the-art competitors.

For comparing the overall performances of the DI + SLIDE and the DI + Hinge, we draw the Pareto-front lines between the DI values and accuracies corresponding to various values of  $\lambda$  in the left side of Figure 4. The lines are the averages taken over five repetitions of learning with five random initials. It is obvious that the SLIDE-surrogate uniformly dominates the hinge-surrogate in that the SLIDE-surrogate provides a better trade-offs between DI and Acc.

### 5.2. Individual fairness

We compare the SLIDE-surrogate and hinge-surrogate fairness constraints for UIF. Table 4 compares the SLIDE-surrogate and the hinge-surrogate fairness constraints as well as the HySLIDE, which indicates that the SLIDE is superior to the hinge for UIF and competitive to the HySLIDE. Recall that the HySLIDE is inferior to the SLIDE in Table 2. The

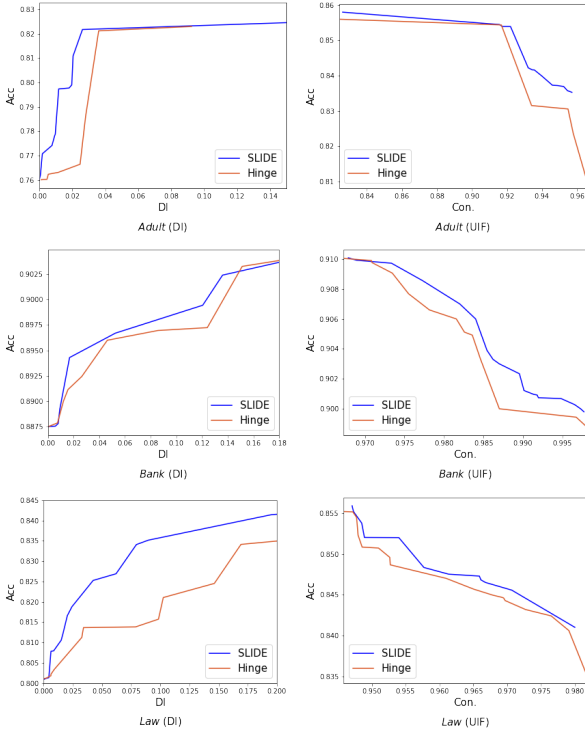


**Figure 4: (Left)** Group fairness (DI) Pareto-front lines between DI and Acc on (upper): *Adult*, (center): *Bank*, and (lower): *Law* test datasets. **(Right)** Individual fairness (UIF) Pareto-front lines between Con. and Acc on (upper): *Adult*, (center): *Bank*, and (lower): *Law* test datasets. These results are averaged on each hyperparameter  $\lambda$ . The blue lines are the results of learned models by the SLIDE-surrogate constraint, and the orange lines are those by the hinge-surrogate constraint.

results in Tables 2 and 4 together imply at least that the SLIDE is not sensitive to the choice of the initial parameters.

Figure 5 draws the Pareto-front lines between the accuracy or the balanced accuracy and a level of fairness, i.e., the consistency (Con.) for the *Adult* dataset, which clearly shows that the SLIDE-surrogate fairness constraint uniformly dominates the hinge-surrogate fairness constraint in that provides a better trade-off.

Table 5 compares two other individual fairness learning algorithms - SenSR (Yurochkin et al. (2020)) and SenSel (Yurochkin and Sun (2020)), i.e., UIF + Linear. Here, we follow the data pre-processing and regularization parameter selection technique used in Yurochkin et al. (2020) and Yurochkin and Sun (2020). In Table 5, S-Con. is the consistency when the variable “spouse” is changed and GR-con. is the consistency when the variables “gender” and “race” are changed (Yurochkin et al. (2020); Yurochkin and Sun (2020)). For these two fairness measures, the SLIDE-surrogate fairness constraint performs better than SenSR and UIF + Linear as well as the hinge-surrogate fairness constraint.

For comparing mean performances on regularization parameter, we also run five experiments with five different initial parameters, and take averages on each  $\lambda$ . Then, we

**Table 4** Individual fairness (UIF) performances (Acc(%), BA(%), Con.) of fair models learned by the SLIDE-surrogate and the hinge-surrogate constraints on *Adult*, *Bank* and *Law* test datasets.

Dataset	Method	Acc	BA	Con.
<i>Adult</i>	UIF + Hinge	84.60	75.75	.916 (.003)
	UIF + SLIDE	84.36	75.73	.920 (.005)
	UIF + HySLIDE	84.51	75.69	<b>.922</b> (.003)
<i>Bank</i>	UIF + Hinge	90.29	63.82	.985 (.006)
	UIF + SLIDE	90.14	63.43	<b>.990</b> (.005)
	UIF + HySLIDE	90.15	63.03	.984 (.004)
<i>Law</i>	UIF + Hinge	83.75	62.67	.985 (.006)
	UIF + SLIDE	83.99	62.71	.986 (.004)
	UIF + HySLIDE	84.02	62.79	<b>.987</b> (.003)

**Table 5** Individual fairness (UIF) performances (Acc(%), BA(%), S-Con., and GR-Con.) of fair models learned by the state-of-the-art baseline methods (UIF + Linear from Yurochkin and Sun (2020) and SenSR from Yurochkin et al. (2020)) on *Adult* test dataset. We copied the results of UIF + Linear and SenSR from Yurochkin and Sun (2020).

<i>Adult</i>	Acc	BA	S-Con.	GR-Con.
UIF + Hinge	85.3	76.8	.936	.967
UIF + SLIDE	85.1	76.6	<b>.970</b>	<b>.985</b>
UIF + HySLIDE	85.2	76.6	<b>.976</b>	.981
UIF + Linear (SenSel)	-	76.8	.945	.963
SenSR	78.7	78.9	.934	<b>.984</b>

compute the Pareto-front lines which is displayed in the right side of Figure 4. It is also observed that the SLIDE-surrogate outperforms the hinge-surrogate in that the SLIDE-surrogate provides a better trade-offs between Con. and Acc.

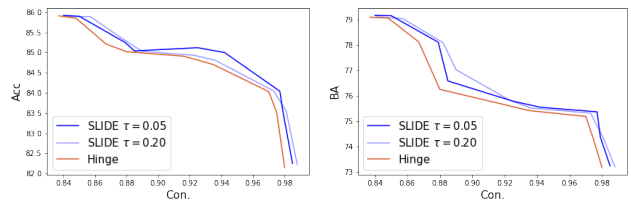


**Figure 5:** Individual fairness (UIF) Pareto-front lines between (left) Con. and Acc, and (right) Con. and BA on *Adult* test dataset. Blue and skyblue lines are those for the SLIDE-surrogate with different  $\tau = 0.05, 0.20$ , and the orange lines are those for the hinge-surrogate.

## 6. Conclusion and discussion

The main message of this paper is to show that using the hinge-surrogate constraint does not provide an optimal prediction model for a given fairness constraint. Thus, we need

to be careful to choose a surrogate fairness constraint, and the choice should depend on the context of a given problem. For example, if the problem is fair classification, one can choose the proposed SLIDE-surrogate fairness constraint, which is theoretically and numerically reasonable.

By closely investigating the gradient of the SLIDE-surrogate fairness constraint, we find an interesting new group fairness constraint so called the *DI-boundary* defined as  $\phi^{\text{DI-bound}}(f) = |\mathbf{P}\{0 \leq f(\mathbf{X}) \leq \tau | Z = 0\} - \mathbf{P}\{0 \leq f(\mathbf{X}) \leq \tau | Z = 1\}|$ . The DI-boundary requires fairness only for individuals whose scores are around the decision boundary. That is, when the fairness of  $f$  is assessed, individuals who have very large scores (i.e., super-performers if a larger value of  $f$  means a higher ability) are excluded from the analysis. If we replace the indicator function in  $\phi^{\text{DI-bound}}(f)$  by the hinge function, the gradient of the hinge-surrogate DI-boundary is equal proportional to the gradient of the SLIDE-surrogate DI provided that  $0 \leq f(\mathbf{X}) \leq \tau$  is replaced by  $0 \leq f^{\text{curr}}(\mathbf{X}) \leq \tau$ , where  $f^{\text{curr}}$  is the current solution. Most existing fairness constraints require a prediction model fair for all individuals. It would be useful to think about the concept of partial fairness, where  $f$  is fair only for a specific subset of the population.

While we have focused on learning fair prediction models, evaluation of the fairness of a given prediction model has also been received much attention (Maity, Xue, Yurochkin and Sun (2021); Awasthi, Beutel, Kleindessner, Morgenstern and Wang (2021)). Specially designed surrogate fairness constraints for the purpose of evaluation of the fairness would be necessary, which we leave as future work.

## Appendix

In this Appendix, we present (i) the proofs of Theorems 1, 2 and 3 in Sections A, B and C, (ii) details of experiments in Section D and (iii) results of additional experiments in Section E.

### A. Notations and definitions

Denote the compact domain of inputs as  $\mathcal{X} \subset \mathbb{R}^d$ . For a given function  $f$ , we let  $\|\cdot\|_p$  be the  $l_p$  norm defined as  $\|f\|_p := (\int_{\mathcal{X}} |f(\mathbf{x})|^p d\mu(\mathbf{x}))^{1/p}$  where  $\mu$  is the Lebesgue measure on  $\mathbb{R}^d$ . In addition, we let  $\|f\|_{\infty} := \sup_{\mathbf{x} \in \mathcal{X}} |f(\mathbf{x})|$ .

For a given  $\alpha > 0$ ,  $[\alpha]$  is the largest integer less than or equal to  $\alpha$  and  $\lceil \alpha \rceil$  is the smallest integer greater or equal to  $\alpha$ . For given  $\mathbf{s} = [s_1, \dots, s_d]^{\top} \in \mathbb{N}_0^d$ , where  $\mathbb{N}_0$  is the set of nonnegative integers, we define the derivative of  $f$  of order  $\mathbf{s}$  as

$$\partial^{\mathbf{s}} f = \frac{\partial^{|\mathbf{s}|} f}{\partial x_1^{s_1} \dots \partial x_d^{s_d}},$$

where  $|\mathbf{s}| = s_1 + \dots + s_d$ . Further, we let

$$[f]_{r, \mathcal{X}} = \sup_{\mathbf{x}, \mathbf{x}' \in \mathcal{X}, \mathbf{x} \neq \mathbf{x}'} \frac{|f(\mathbf{x}) - f(\mathbf{x}')|}{\|\mathbf{x} - \mathbf{x}'\|^r}$$

for  $r \in (0, 1]$ .

**Definition 1** (Smooth functions). For  $m \in \mathbb{N}$ , we denote  $C^m(\mathcal{X})$  as the space of  $m$ -times differentiable functions on  $\mathcal{X}$  as whose partial derivatives of order  $\mathbf{s}$  with  $|\mathbf{s}| \leq m$  are continuous. That is,

$$C^m(\mathcal{X}) = \{f : \mathcal{X} \rightarrow \mathbb{R},$$

$$\partial^{\mathbf{s}} f \text{ are continuous for } \forall \mathbf{s} \text{ such that } |\mathbf{s}| \leq m\}.$$

**Definition 2** (Hölder space). Hölder space with smoothness  $\zeta > 0$  is a function space defined as

$$\mathcal{H}^{\zeta}(\mathcal{X}) := \{f \in C^{\lceil \zeta \rceil}(\mathcal{X}) : \|f\|_{\mathcal{H}^{\zeta}(\mathcal{X})} < \infty\}$$

where

$$\|f\|_{\mathcal{H}^{\zeta}(\mathcal{X})} = \max_{|\mathbf{m}| \leq \lceil \zeta \rceil} \|\partial^{\mathbf{m}} f\|_{\infty, \mathcal{X}} + \max_{|\mathbf{m}| = \lceil \zeta \rceil} [\partial^{\mathbf{m}} f]_{\zeta_0, \mathcal{X}}.$$

**Definition 3** (The  $\epsilon$ -covering number). The  $\epsilon$ -covering number of a given class of functions  $\mathcal{F}$  is the cardinality of the minimal  $\epsilon$ -covering set of  $\mathcal{F}$  with respect to the  $L_p$  norm, which is defined as:

$$N(\epsilon, \mathcal{F}, \|\cdot\|_p) :=$$

$$\inf \{n \in \mathbb{N} : \exists f_1, \dots, f_n \text{ s.t. } \mathcal{F} \subset \bigcup_{i=1}^n B_p(f_i, \epsilon)\},$$

where  $B_p(f_i, \epsilon) := \{f \in \mathcal{F} : \|f - f_i\|_p \leq \epsilon\}$ .

**Definition 4** (Metric entropy). The ( $\epsilon$ -) metric entropy of  $\mathcal{F}$  (w.r.t.  $L_p$  norm) is a logarithm of the  $\epsilon$ -covering number of  $\mathcal{F}$  (w.r.t.  $L_p$  norm), i.e.,

$$H(\epsilon, \mathcal{F}, \|\cdot\|_p) := \log(N(\epsilon, \mathcal{F}, \|\cdot\|_p)).$$

**Definition 5** (Rademacher complexity). Let  $\sigma$  be a random variable having -1 or 1 with probability 1/2 each. For independent realizations  $\sigma_1, \dots, \sigma_n$  of  $\sigma$ , we define the empirical Rademacher complexity of a function class  $\mathcal{F}$  as

$$\hat{\mathcal{R}}(\mathcal{F}) := \frac{1}{n} \mathbf{E}_{\sigma} \left( \sup_{f \in \mathcal{F}} \sum_{i=1}^n \sigma_i f(\mathbf{X}_i) \right).$$

The Rademacher complexity is the expectation of the empirical one with respect to  $\mathbf{X}$ . That is, the (population) Rademacher complexity of  $\mathcal{F}$  is

$$\mathcal{R}(\mathcal{F}) := \mathbf{E}_{\mathbf{X}} \left( \hat{\mathcal{R}}(\mathcal{F}) \right).$$

### B. Technical lemmas

This section introduces technical lemmas used to prove the Theorems 1, 2 and 3. Particularly, Lemma 5 provides a tight upper bound of  $\hat{\mathcal{R}}(\mathcal{V}_{\tau}(\mathcal{F}))$  when  $\mathcal{F}$  is class of deep neural networks, which plays a key role in deriving the convergence rates. In addition, even though we do not derive the convergence rates, we demonstrate how to obtain a tight upper bound of  $\hat{\mathcal{R}}(\mathcal{V}_{\tau}(\mathcal{F}))$  when  $\mathcal{F}$  is a class of linear functions in Example 1. For technical simplicity, we assume that the distribution of  $\mathbf{X}$  has a density  $p(\mathbf{x})$  such that  $0 < \inf_{\mathbf{x} \in \mathcal{X}} p(\mathbf{x}) \leq \sup_{\mathbf{x} \in \mathcal{X}} p(\mathbf{x}) < \infty$ .

**Lemma 1.** Let  $\eta_f(\mathbf{x}) := D(f(\mathbf{x}), f(\mathbf{x}')) - \gamma$  with a Lipschitz (on bounded domain) metric  $D(\cdot, \cdot)$  for a given  $\gamma > 0$ . Then, there exists  $c > 0$  such that

$$\|\eta_{f_1} - \eta_{f_2}\|_\infty \leq c \|f_1 - f_2\|_\infty$$

for any two functions  $f_1$  and  $f_2$ .

**Lemma 2** (Theorem 26.5 of Shalev-Shwartz and Ben-David (2014)). Let  $\mathcal{H}$  be a set of real-valued functions such that  $\|l \circ h\|_\infty \leq H$  for any  $h \in \mathcal{H}$  for some  $H > 0$ . Then,

$$L_P(h) \leq L_n(h) + 2\hat{\mathcal{R}}_n(l \circ \mathcal{H}) + 4H \sqrt{\frac{2 \log(4/\delta)}{n}}$$

for any  $h \in \mathcal{H}$ , with probability at least  $1 - \delta > 0$ .

**Lemma 3** (Dudley's Theorem (Theorem 1.19 of Wolf (2018))). Let  $\mathcal{H}$  be a set of real-valued functions such that  $\|h\|_\infty \leq H$  for any  $h \in \mathcal{H}$  for some  $H > 0$ . Then,

$$\hat{\mathcal{R}}(\mathcal{H}) \leq \inf_{\alpha \in [0, \frac{H}{2})} \left( 4\alpha + \frac{12}{\sqrt{n}} \int_\alpha^H \sqrt{\log \mathcal{N}(\epsilon, \mathcal{H}, \|\cdot\|_{n,2})} d\epsilon \right) \quad (7)$$

where  $\|\cdot\|_{n,2}$  denotes the empirical  $L_2$  norm defined by  $\|h\|_{n,2} := \sqrt{n^{-1} \sum_{i=1}^n h(\mathbf{X}_i)^2}$  for  $h \in \mathcal{H}$ .

**Lemma 4** (Lemma 3 of Suzuki (2019)). Let  $\mathcal{F}$  be a set of deep neural networks with the ReLU activation function,  $L$  many layers,  $N$  many nodes at each layer,  $S$  many nonzero weights and biases that are bounded by  $B$ . Then for any  $\epsilon > 0$ ,

$$\log \mathcal{N}(\epsilon, \mathcal{F}, \|\cdot\|_\infty) \leq 2S(L+1) \log \left( \frac{(L+1)(N+1)B}{\epsilon} \right). \quad (8)$$

**Lemma 5.** Let  $g : \mathbb{R} \rightarrow \mathbb{R}$  be a Lipschitz function in a sense that  $|g(z_1) - g(z_2)| \leq C'|z_1 - z_2|$  for any  $z_1, z_2 \in \mathbb{R}$  for some constant  $C' > 0$ . Let  $\mathcal{F}$  be a set of deep neural networks with the ReLU activation function,  $L$  many layers,  $N$  many nodes at each layer,  $S$  many nonzero weights and biases that are bounded by  $B$ . Let  $g(\mathcal{F}) := \{g(f) : f \in \mathcal{F}\}$  and  $F' = \sup_{f \in \mathcal{F}} \|g(f)\|_\infty$ . Then

$$\hat{\mathcal{R}}(g(\mathcal{F})) \leq \frac{4}{n} + \frac{12F'}{\sqrt{n}} \sqrt{S(L+1) \log(C'n(L+1)(N+1)B)}.$$

The next two propositions compute  $M_{n,f}$  for UIF and DI.

**Proposition 1** (Upper bound of  $M_f$  for UIF). Let  $\mathcal{F}$  be the class of DNN models considered in Theorem 3. Suppose  $\tau_n = \mathcal{O}(b_n)$ , where  $b_n$  is the sequence defined in Theorem 3. Then we have

$$M_f \leq \frac{1}{\tau_n} |\phi_{n, \tau_n}^{\text{slide}}(f; \gamma, \epsilon) - \phi_{n, \tau_n}^{\text{slide}}(f; \gamma, \epsilon)| + \mathcal{O}(1)$$

for all  $f \in \mathcal{F}$ .

**Proposition 2** (Upper bound of  $M_f$  for DI). Let  $\mathcal{F}$  be the class of DNN models considered in Theorem 3. Suppose  $\tau_n = \mathcal{O}(b_n)$ , where  $b_n$  is the sequence defined in Theorem 3. Then we have for all  $f \in \mathcal{F}$ ,

$$M_f \leq \frac{1}{\tau_n} \sum_{z=0,1} \left| \frac{1}{n_z} \sum_{z_i=z} \left( v_{-\tau_n}(f(\mathbf{x}_i)) - v_{\tau_n}(f(\mathbf{x}_i)) \right) \right| + \frac{1}{\tau_n} |\phi_{n, \tau_n}^{\text{slide}}(f) - \phi_n(f)| + \mathcal{O}(1).$$

Obtaining a tight upper bound of the Rademacher complexity plays a key role to derive a fast convergence rate. We need an upper bound of  $\hat{\mathcal{R}}(v_\tau(\mathcal{F}))$  while that of  $\hat{\mathcal{R}}(\mathcal{F})$  is well known for many classes of  $\mathcal{F}$ . Since  $v_\tau$  is  $1/\tau$ -Lipschitz, we may use the inequality  $\hat{\mathcal{R}}(v_\tau(\mathcal{F})) \leq \hat{\mathcal{R}}(\mathcal{F})/\tau$  to derive an upper bound. However, such a naive approach would not yield a good upper bound in particular when  $\tau$  converges to 0 as  $n$  increases. For DNNs, we derive an upper bound in Lemma 5 by directly calculating the corresponding metric entropy. In the following example, we illustrate how to derive a good upper bound of the Rademacher complexity when  $\mathcal{F}$  is a class of linear functions. In particular, we derive an upper bound of the  $L_2$ -metric entropy of  $v_\tau(\mathcal{F})$ , with which we could obtain an upper bound of the Rademacher complexity by use of Lemma 3.

**Example 1** (Linear model  $\mathcal{F}^{\text{linear}}$ ). Let  $\mathcal{F}^{\text{linear}} = \{\langle \mathbf{w}, \cdot \rangle : \mathbf{w} \in \mathbb{R}^d, \|\mathbf{w}\|_2 \leq B\}$ . Since  $v_\tau$  is  $1/\tau$ -Lipschitz, we have  $\mathcal{N}(\epsilon, v_\tau(\mathcal{F}^{\text{linear}}), \|\cdot\|_2) \leq \mathcal{N}(\epsilon\tau, \mathcal{F}^{\text{linear}}, \|\cdot\|_\infty)$ . Finally, we can obtain the bound of the entropy as  $\log \mathcal{N}(\epsilon\tau_n, \mathcal{F}^{\text{linear}}, \|\cdot\|_\infty) \leq d \log \left( \frac{C}{\epsilon\tau_n} \right)$  for some  $C > 0$  and  $\tau = \tau_n$  by Lemma 2.5 of van de Geer (2000). Hence, the Rademacher complexity of  $v_{\tau_n}(\mathcal{F}^{\text{linear}})$  is bounded by (asymptotically)  $\log(1/\tau_n)$  but not  $1/\tau_n$ .

## C. Proofs

This section presents the proofs of Lemmas 1 and 5, Theorems 1, 2 and 3, and Propositions 1 and 2.

### Proof of Lemma 1

*Proof.* By the Lipschitz property of  $D$ , there exists a constant  $C > 0$  such that  $D(z, z') \leq C|z - z'|$  for all  $z, z' \in \{x \in \mathbb{R} : |x| \leq K\}$ , which is a bounded domain, for a given  $K > 0$ .

Denote

$$\mathbf{x}'_{f_1} := \arg \max_{\mathbf{x}' : d(\mathbf{x}, \mathbf{x}') \leq \epsilon} D(f_1(\mathbf{x}), f_1(\mathbf{x}'))$$

and

$$\mathbf{x}'_{f_2} := \arg \max_{\mathbf{x}' : d(\mathbf{x}, \mathbf{x}') \leq \epsilon} D(f_2(\mathbf{x}), f_2(\mathbf{x}')).$$

Then, we consider any metric as the similarity measure  $D(\cdot, *)$  between prediction values, we can write  $|\eta_{f_1}(\mathbf{x}) - \eta_{f_2}(\mathbf{x})| = |D(f_1(\mathbf{x}), f_1(\mathbf{x}'_{f_1})) - D(f_2(\mathbf{x}), f_2(\mathbf{x}'_{f_2}))|$ .

(Case 1)  $D(f_1(\mathbf{x}), f_1(\mathbf{x}'_{f_1})) \geq D(f_2(\mathbf{x}), f_2(\mathbf{x}'_{f_2}))$  : Then,

$$\begin{aligned} |\eta_{f_1}(\mathbf{x}) - \eta_{f_2}(\mathbf{x})| &= D(f_1(\mathbf{x}), f_1(\mathbf{x}'_{f_1})) - D(f_2(\mathbf{x}), f_2(\mathbf{x}'_{f_2})) \\ &\leq D(f_1(\mathbf{x}), f_1(\mathbf{x}'_{f_1})) - D(f_2(\mathbf{x}), f_2(\mathbf{x}'_{f_1})) \\ &\leq \left| D(f_1(\mathbf{x}), f_1(\mathbf{x}'_{f_1})) - D(f_2(\mathbf{x}), f_2(\mathbf{x}'_{f_1})) \right| \\ &\leq D(f_1(\mathbf{x}), f_2(\mathbf{x})) + D(f_1(\mathbf{x}'_{f_1}), f_2(\mathbf{x}'_{f_1})). \end{aligned}$$

The first inequality holds since

$$D(f_2(\mathbf{x}), f_2(\mathbf{x}'_{f_2})) \geq D(f_2(\mathbf{x}), f_2(\mathbf{x}'))$$

for all  $\mathbf{x}'$ .

(Case 2)  $D(f_1(\mathbf{x}), f_1(\mathbf{x}'_{f_1})) \leq D(f_2(\mathbf{x}), f_2(\mathbf{x}'_{f_2}))$  :

We can derive  $|\eta_{f_1}(\mathbf{x}) - \eta_{f_2}(\mathbf{x})| \leq D(f_1(\mathbf{x}), f_2(\mathbf{x})) + D(f_1(\mathbf{x}'_{f_1}), f_2(\mathbf{x}'_{f_2}))$  similarly.

Since the two inequalities hold for any  $\mathbf{x}$  and  $D$  is Lipschitz, we can take supremum for each hand-side:

$$\begin{aligned} \|\eta_{f_1} - \eta_{f_2}\|_\infty &= \sup_{\mathbf{x}} |\eta_{f_1}(\mathbf{x}) - \eta_{f_2}(\mathbf{x})| \\ &\leq 3 \sup_{\mathbf{x}} D(f_1(\mathbf{x}), f_2(\mathbf{x})) \\ &\leq 3C \sup_{\mathbf{x}} \|f_1(\mathbf{x}) - f_2(\mathbf{x})\| \\ &= c \|f_1 - f_2\|_\infty \end{aligned}$$

where  $c = 3C$ . Here, we note that the first inequality holds by the inequality  $|\eta_{f_1}(\mathbf{x}) - \eta_{f_2}(\mathbf{x})| \leq D(f_1(\mathbf{x}), f_2(\mathbf{x})) + D(f_1(\mathbf{x}'_{f_1}), f_2(\mathbf{x}'_{f_2})) + D(f_2(\mathbf{x}'_{f_2}), f_2(\mathbf{x}'_{f_1}))$  using (Case 1) and (Case 2). It finally implies the desired result that

$$\|\eta_{f_1} - \eta_{f_2}\|_\infty \leq c \|f_1 - f_2\|_\infty$$

holds for some  $c > 0$  that only depends on the Lipschitz constant  $C$ .  $\square$

### Proof of Lemma 5

*Proof.* By the Lipschitz property of  $g$ , we have  $\|g(f_1) - g(f_2)\|_{n,2}^2 = \frac{1}{n} \sum_{i=1}^n |g(f_1(\mathbf{x}_i)) - g(f_2(\mathbf{x}_i))|^2 \leq (C')^2 \|f_1 - f_2\|_{n,2}^2$  and thus  $\mathcal{N}(\epsilon, g(\mathcal{F}), \|\cdot\|_{n,2}) \leq \mathcal{N}(\epsilon/C', \mathcal{F}, \|\cdot\|_\infty)$ . Then by Lemma 4, the integral term in Lemma 3 is bounded as

$$\begin{aligned} &\int_\alpha^{F'} \sqrt{\log \mathcal{N}(u/C', \mathcal{F}, \|\cdot\|_\infty)} d\epsilon \\ &\leq F' \sqrt{\log \mathcal{N}(\alpha/C', \mathcal{F}, \|\cdot\|_\infty)} \\ &\leq F' \sqrt{2S(L+1) \log \left( \frac{C'(L+1)(N+1)B}{\alpha} \right)}. \end{aligned}$$

Taking  $\alpha = 1/n$  completes the proof.  $\square$

### Proof of Theorem 1

*Proof.* Let

$$\phi_{\tau_n}^{\text{slide}}(f) = |\mathbf{E}\{v_{\tau_n}(f(\mathbf{X}))|Z=0\} - \mathbf{E}\{v_{\tau_n}(f(\mathbf{X}))|Z=1\}|.$$

Then using the inequality  $|a| - |b| \leq |a - b|$ , we have that

$$\begin{aligned} &\left| \phi_{n,\tau_n}^{\text{slide}}(\hat{f}_n) - \phi(\hat{f}_n) \right| - \left| \phi_{\tau_n}^{\text{slide}}(\hat{f}_n) - \phi(\hat{f}_n) \right| \\ &\leq \left| \phi_{n,\tau_n}^{\text{slide}}(\hat{f}_n) - \phi_{\tau_n}^{\text{slide}}(\hat{f}_n) \right| \\ &= \left| \frac{1}{n_0} \sum_{i:z_i=0} v_{\tau_n}(\hat{f}_n(\mathbf{x}_i)) - \frac{1}{n_1} \sum_{i:z_i=1} v_{\tau_n}(\hat{f}_n(\mathbf{x}_i)) \right| \\ &\quad - \left| \mathbf{E}\{v_{\tau_n}(\hat{f}_n(\mathbf{X}))|Z=0\} - \mathbf{E}\{v_{\tau_n}(\hat{f}_n(\mathbf{X}))|Z=1\} \right| \\ &\leq \left| \frac{1}{n_0} \sum_{i:z_i=0} v_{\tau_n}(\hat{f}_n(\mathbf{x}_i)) - \mathbf{E}\{v_{\tau_n}(\hat{f}_n(\mathbf{X}))|Z=0\} \right| \\ &\quad + \left| \frac{1}{n_1} \sum_{i:z_i=1} v_{\tau_n}(\hat{f}_n(\mathbf{x}_i)) - \mathbf{E}\{v_{\tau_n}(\hat{f}_n(\mathbf{X}))|Z=1\} \right| \\ &= \sum_{z \in \{0,1\}} \left| \frac{1}{n_z} \sum_{i:z_i=z} v_{\tau_n}(\hat{f}_n(\mathbf{x}_i)) - \mathbf{E}\{v_{\tau_n}(\hat{f}_n(\mathbf{X}))|Z=z\} \right|. \end{aligned}$$

Since the SLIDE function  $v_{\tau_n}$  is bounded in  $[0, 1]$ , by Lemma 2 the first term of the right-hand side of the preceding display is bounded by

$$\sum_{z \in \{0,1\}} \left( \hat{\mathcal{R}}_z(v_{\tau_n}(\mathcal{F})) + 4\sqrt{\frac{2 \log(8n)}{n_z}} \right)$$

with probability at least  $1 - 1/n$ . On the other hand, the second term of the right-hand side is bounded by  $M_{\hat{f}_n} \tau_n$  by the definition of  $M_f$ . By the assumptions  $n_1/n_0 \rightarrow s \in (0, \infty)$ , we have

$$\begin{aligned} \phi(\hat{f}_n) &\leq \phi_{n,\tau_n}^{\text{slide}}(\hat{f}_n) + \left| \phi_{n,\tau_n}^{\text{slide}}(\hat{f}_n) - \phi(\hat{f}_n) \right| \\ &\leq \alpha + \delta_n + C \left( \sum_{z \in \{0,1\}} \hat{\mathcal{R}}_z(v_{\tau_n}(\mathcal{F})) + \sqrt{\frac{\log n}{n}} \right) \\ &\quad + M_{\hat{f}_n} \tau_n \end{aligned}$$

for some constant  $C > 0$  with probability at least  $1 - 1/n$ , which completes the proof.  $\square$

### Proof of Theorem 2

*Proof.* Let  $\phi_{\tau_n}^{\text{slide}}(f; \gamma, \epsilon) = \mathbb{E}\{v_{\tau_n} \circ \eta_f\}$ . Since the SLIDE function  $v_{\tau_n}$  is bounded in  $[0, 1]$ , Lemma 2 implies that

$$\begin{aligned} &\left| \phi_{n,\tau_n}^{\text{slide}}(\hat{f}_n; \gamma, \epsilon) - \phi(\hat{f}_n; \gamma, \epsilon) \right| \\ &\leq \left| \phi_{n,\tau_n}^{\text{slide}}(\hat{f}_n; \gamma, \epsilon) - \phi_{\tau_n}^{\text{slide}}(\hat{f}_n; \gamma, \epsilon) \right| \\ &\quad + \left| \phi_{\tau_n}^{\text{slide}}(\hat{f}_n; \gamma, \epsilon) - \phi(\hat{f}_n; \gamma, \epsilon) \right| \\ &\leq 2\hat{\mathcal{R}}(v_{\tau_n} \circ \eta(\mathcal{F})) + 4\sqrt{\frac{2 \log(4n)}{n}} + M_{\hat{f}_n} \tau_n \end{aligned}$$

with probability at least  $1 - 1/n$ , which completes the proof.  $\square$

### Proof of Theorem 3

*Proof.* We prove Theorem 3 for DI and UIF separately.

**(Case 1: DI)** Since  $f_\alpha^*$  is a Hölder smooth function with smoothness  $\zeta > 0$ , by Theorem 5 of Schmidt-Hieber et al. (2020), for any sufficiently large  $n$ , there is a neural network  $f_n^* \in \mathcal{F}$  such that

$$\|f_n^* - f_\alpha^*\|_\infty \leq C'_1 n^{-\frac{\zeta}{2\zeta+d}} =: b'_n$$

for some absolute constant  $C'_1 > 0$ , provided that  $L_n = L_0 \log n$ ,  $N_n = N_0 n^{\frac{d}{2\zeta+d}}$ ,  $S_n = S_0 n^{\frac{d}{2\zeta+d}} \log n$ ,  $B_n = 1$  and  $F_n = F_0 \geq \|f_\alpha^*\|_\infty$ , where  $L_0, N_0, S_0$  and  $F_0$  are constants depending only on  $d$  and  $\zeta$ . From now on, we assume that the set  $\mathcal{F}$  include all deep neural networks of the architectures satisfying the above conditions. By the Lipschitz property of  $\phi$ , we have

$$\phi(f_n^*) \leq \phi(f_\alpha^*) + L \|f_n^* - f_\alpha^*\|_\infty \leq \alpha + M b'_n$$

i.e.,  $f_n^* \in \mathcal{F}_{\alpha + M b'_n}$ . Define the event

$$\mathcal{E}_n(\xi) := \left\{ \{(Y_i, \mathbf{X}_i)\}_{i=1}^n : \sup_{f \in \mathcal{F}} |\phi_{n, \tau_n}^{\text{slide}}(f) - \phi(f)| \leq \xi \right\}$$

for  $\xi > 0$ . Let

$$\phi_{\tau_n}^{\text{slide}}(f) = |\mathbf{E}(v_{\tau_n}(f(\mathbf{X}))|Z=0) - \mathbf{E}(v_{\tau_n}(f(\mathbf{X}))|Z=1)|.$$

Then using the inequality  $|a| - |b| \leq |a - b|$ , we get

$$\begin{aligned} & \left| \phi_{n, \tau_n}^{\text{slide}}(\hat{f}_n) - \phi(\hat{f}_n) \right| \\ & \leq \sum_{z \in \{0,1\}} \left| \frac{1}{n_z} \sum_{i: z_i=z} v_{\tau_n}(\hat{f}_n(\mathbf{x}_i)) - \mathbf{E}(v_{\tau_n}(\hat{f}_n(\mathbf{X}))|Z=z) \right| \\ & \quad + |\phi_{\tau_n}^{\text{slide}}(\hat{f}_n) - \phi(\hat{f}_n)|. \end{aligned}$$

Since the SLIDE function  $v_{\tau_n}$  is  $1/\tau_n$ -Lipschitz and bounded in  $[0, 1]$ , by Lemmas 2 and 5, the first term of the right-hand side of the preceding display is bounded as

$$\begin{aligned} & \sum_{z \in \{0,1\}} \frac{8}{n_z} \\ & + \sum_{z \in \{0,1\}} \frac{24}{\sqrt{n_z}} \sqrt{S_n(L_n + 1) \log \frac{n(L_n + 1)(N_n + 1)B_n}{\tau_n}} \\ & + \sum_{z \in \{0,1\}} 4 \sqrt{\frac{2 \log(4/\delta)}{n_z}} \\ & \leq C'_2 \sum_{z \in \{0,1\}} \left( \frac{1}{n_z} + \sqrt{\frac{\frac{p}{n^{2\zeta+p}} (\log n)^3}{n_z}} + \sqrt{\frac{\log(1/\delta)}{n_z}} \right) \end{aligned}$$

for some constant  $C'_2 > 0$  with probability at least  $1 - 2\delta$ . On the other hand, the second term of the right-hand side is bounded by  $M_{\hat{f}_n} \tau_n$  by the definition of  $M_f$ . Hence, by the assumptions  $n_1/n_0 \rightarrow s \in (0, \infty)$ , we have by taking  $\delta = 1/(8n)$ ,

$$\begin{aligned} & \left| \phi_{n, \tau_n}^{\text{slide}}(\hat{f}_n) - \phi(\hat{f}_n) \right| \\ & \leq C'_3 \left( n^{-\frac{\zeta}{2\zeta+p}} (\log n)^{3/2} \right) = C'_3 b_n + M_{\hat{f}_n} \tau_n \end{aligned}$$

for some constant  $C'_3 > 0$  with probability at least  $1 - 1/(4n)$ . That is,  $\mathbf{P}\{\mathcal{E}_n(C'_3 b_n + M_{\hat{f}_n} \tau_n)^c\} \leq 1/(4n)$ .

Now we show that the convergence rate of  $\mathcal{E}(\hat{f}_n, f_n^*)$  on  $\mathcal{E}_n(C'_3 b_n + M_{\hat{f}_n} \tau_n)$ . Firstly we note that on  $\mathcal{E}(C'_3 b_n + M_{\hat{f}_n} \tau_n)$ ,  $f_n^* \in \mathcal{F}_{n, \alpha + M b'_n + C'_3 b_n + M_{\hat{f}_n} \tau_n, \tau_n}$ .

Thus, since  $\hat{f}_n$  is the ERM over  $\mathcal{F}_{n, \alpha + \delta_n}$ , where  $\delta_n > C_2 b_n > M b'_n + C'_3 b_n + M_{\hat{f}_n} \tau_n$  for sufficiently large  $C_2 > 0$  by assumption and  $\mathbf{P}\{\mathcal{E}_n(C'_3 b_n + M_{\hat{f}_n} \tau_n)\} \geq 1 - 1/(4n)$ , we have

$$\begin{aligned} \mathcal{E}(\hat{f}_n, f_n^*) & \leq L(\hat{f}_n) - L(f_n^*) - L_n(\hat{f}_n) + L_n(f_n^*) \\ & \leq 2\mathcal{R}(g(\mathcal{F})) + 4(\log 2 + 2F_0) \sqrt{\frac{2 \log(8n)}{n}} \end{aligned}$$

with probability at least  $1 - 1/(2n)$ , where we denote  $L(f) = \mathbf{E}\{l(Y, f(\mathbf{X}))\}$ . Here, we let  $g(f) := l(Y, f(\mathbf{X})) - l(Y, f_n^*(\mathbf{X}))$  and  $g(\mathcal{F}) := \{g(f) : f \in \mathcal{F}\}$ . The second inequality follows from the Rademacher complexity bound in Lemma 2 with the fact that  $|g(f)| \leq (\log 2 + 2F_0)$  for any  $f \in \mathcal{F}$ . Moreover, since  $|g(f_1) - g(f_2)| \leq |f_1(\mathbf{X}) - f_2(\mathbf{X})|$  for any  $(\mathbf{X}, Y)$  due to the Lipschitz property of the logistic loss  $l$ , by Lemma 5, the preceding display is further bounded by

$$\frac{1}{\sqrt{n}} \sqrt{\frac{d}{n^{2\zeta+d}} (\log n)^3} = n^{-\frac{\zeta}{2\zeta+d}} (\log n)^{3/2} = b_n$$

up to some multiplicative constant. Therefore, there is a constant  $C'_4 > 0$  such that

$$\begin{aligned} & \mathbf{P}\{\mathcal{E}(\hat{f}_n, f_n^*) > C'_4 b_n + M_{\hat{f}_n} \tau_n\} \\ & \leq \mathbf{P}\{\mathcal{E}(\hat{f}_n, f_n^*) > (C'_4/2) b_n + M_{\hat{f}_n} \tau_n\} \\ & \quad + \mathbf{P}\{\mathcal{E}(f_n^*, f_n^*) > (C'_4/2) b_n + M_{\hat{f}_n} \tau_n\} \\ & \leq \mathbf{P}\{\{\mathcal{E}(\hat{f}_n, f_n^*) > (C'_4/2) b_n\} \cap \mathcal{E}_n(C'_3 b_n + M_{\hat{f}_n} \tau_n)\} \\ & \quad + \mathbf{P}\{\mathcal{E}_n(C'_3 b_n + M_{\hat{f}_n} \tau_n)^c\} \\ & \quad + \mathbf{P}\{\|f_n^* - f_\alpha^*\|_\infty > (C'_4/2) b_n + M_{\hat{f}_n} \tau_n\} \\ & \leq 1 - n^{-1}, \end{aligned}$$

which completes the proof of the first assertion.

The second assertion follows from the fact that on  $\mathcal{E}_n(C'_3 b_n + M_{\hat{f}_n} \tau_n)$ ,

$$\begin{aligned} \phi(\hat{f}_n) & \leq \phi_{n, \tau_n}^{\text{slide}}(\hat{f}_n) + C'_3 b_n + M_{\hat{f}_n} \tau_n \\ & \leq \alpha + \delta_n + C'_3 b_n + M_{\hat{f}_n} \tau_n. \end{aligned}$$

(Case 2: UIF) The proof is almost the same as that of (Case 1: DI). The only difference is that we need to derive bounds of the Rademacher complexity  $\widehat{\mathcal{R}}(\nu_{\tau_n} \circ \eta(\mathcal{F}))$  and the term

$$\left| \phi_{\tau_n, \tau_n}^{\text{slide}}(\widehat{f}_n; \gamma, \epsilon) - \phi(\widehat{f}_n; \gamma, \epsilon) \right|.$$

By Lemma 1,

$$|\nu_{\tau_n} \circ \eta_{f_1}(\mathbf{x}) - \nu_{\tau_n} \circ \eta_{f_2}(\mathbf{x})| \leq \frac{C'_1}{\tau_n} \|f_1 - f_2\|_\infty$$

for any  $f_1, f_2$  and any  $\mathbf{x}$  for some  $C'_1 > 0$ . Therefore, we have that

$$\begin{aligned} \widehat{\mathcal{R}}(\nu_{\tau_n} \circ \eta(\mathcal{F})) &\leq \frac{4}{n} + \\ &\frac{12}{\sqrt{n}} \sqrt{S_n(L_n + 1) \log \frac{n(L_n + 1)(N_n + 1)B_n}{\tau_n}} \\ &\leq C'_2 n^{-\frac{\xi}{2\xi+d}} (\log n)^{3/2} = C'_2 b_n \end{aligned}$$

for some constant  $C'_2 > 0$ . In turn, similarly to the proof of (Case 1: DI), we have

$$\begin{aligned} \left| \phi_{\tau_n, \tau_n}^{\text{slide}}(\widehat{f}_n; \gamma, \epsilon) - \phi(\widehat{f}_n; \gamma, \epsilon) \right| &\leq 2\widehat{\mathcal{R}}(\nu_{\tau_n} \circ \eta(\mathcal{F})) \\ &\quad + 4\sqrt{\frac{2 \log(4n)}{n}} \\ &\quad + M_{\widehat{f}_n} \tau_n \\ &\leq M_{\widehat{f}_n} \tau_n + C'_4 b_n \end{aligned}$$

with probability  $1 - 1/(4n)$  for some constant  $C'_4 > 0$ . Finally, we can complete the proof similarly to the proof of (Case 1: DI).  $\square$

### Proof of Proposition 1

*Proof.* Note that  $|\phi(f; \gamma, \epsilon) - \phi_{\tau_n}^{\text{slide}}(f; \gamma, \epsilon)| \leq |\phi_{\tau_n}^{\text{slide}}(f; \gamma, \epsilon) - \phi_{-\tau_n}^{\text{slide}}(f; \gamma, \epsilon)|$ . By triangle inequality, we obtain

$$\begin{aligned} &|\phi_{\tau_n}^{\text{slide}}(f; \gamma, \epsilon) - \phi_{-\tau_n}^{\text{slide}}(f; \gamma, \epsilon)| \\ &\leq |\phi_{\tau_n}^{\text{slide}}(f; \gamma, \epsilon) - \phi_{n, \tau_n}^{\text{slide}}(f; \gamma, \epsilon)| \\ &\quad + |\phi_{-\tau_n}^{\text{slide}}(f; \gamma, \epsilon) - \phi_{n, -\tau_n}^{\text{slide}}(f; \gamma, \epsilon)| \\ &\quad + |\phi_{n, \tau_n}^{\text{slide}}(f; \gamma, \epsilon) - \phi_{n, -\tau_n}^{\text{slide}}(f; \gamma, \epsilon)|. \end{aligned}$$

The first and second terms can be bounded as below using Lemmas 2 and 5 using the same arguments used in the proof of Theorem 3. That is, since the SLIDE functions  $\nu_{\tau_n}$  and  $\nu_{-\tau_n}$  are  $1/\tau_n$ -Lipschitz and bounded in  $[0, 1]$ , the first two terms are bounded by

$$\begin{aligned} &C' \left( \frac{1}{n} + \frac{1}{\sqrt{n}} \sqrt{S_n(L_n + 1) \log \frac{n(L_n + 1)(N_n + 1)B_n}{\tau_n}} \right) \\ &\quad + 4\sqrt{\frac{2 \log(1/(2\delta))}{n}} \end{aligned}$$

$$\leq C \left( \frac{1}{n} + \frac{1}{\sqrt{n}} \sqrt{n^{\frac{p}{2\xi+p}} (\log n)^3} + \sqrt{\frac{\log(1/\delta)}{n}} \right)$$

for some constant  $C', C > 0$  with probability at least  $1 - 2\delta$ .

Now let  $b_n = n^{-\frac{\xi}{2\xi+d}} (\log n)^{3/2}$  up to constant with  $\delta = 1/8n$  as is done in Theorem 3. Then we obtain that

$$|\phi_{\tau_n}^{\text{slide}}(f; \gamma, \epsilon) - \phi_{n, \tau_n}^{\text{slide}}(f; \gamma, \epsilon)| = \mathcal{O}(b_n)$$

and

$$|\phi_{-\tau_n}^{\text{slide}}(f; \gamma, \epsilon) - \phi_{n, -\tau_n}^{\text{slide}}(f; \gamma, \epsilon)| = \mathcal{O}(b_n).$$

Thus we conclude

$$|\phi_{\tau_n}^{\text{slide}}(f; \gamma, \epsilon) - \phi_{-\tau_n}^{\text{slide}}(f; \gamma, \epsilon)|$$

$$\leq |\phi_{n, \tau_n}^{\text{slide}}(f; \gamma, \epsilon) - \phi_{n, -\tau_n}^{\text{slide}}(f; \gamma, \epsilon)| + \mathcal{O}(b_n)$$

and dividing by  $\tau_n$  completes the proof.  $\square$

### Proof of Proposition 2

*Proof.* By triangle inequality,  $|\phi(f) - \phi_{\tau_n}^{\text{slide}}(f)| \leq |\phi_{\tau_n}^{\text{slide}}(f) - \phi_{n, \tau_n}^{\text{slide}}(f)| + |\phi(f) - \phi_n(f)| + |\phi_{n, \tau_n}^{\text{slide}}(f) - \phi_n(f)|$ . The first term is bounded as below using Lemmas 2 and 5 by the same arguments used in the proof of Theorem 3. That is, since the SLIDE function  $\nu_{\tau_n}$  are  $1/\tau_n$ -Lipschitz and bounded in  $[0, 1]$ , it is bounded by

$$\begin{aligned} &\sum_{z \in \{0,1\}} \frac{8}{n_z} \\ &\quad + \sum_{z \in \{0,1\}} \frac{24}{\sqrt{n_z}} \sqrt{S_n(L_n + 1) \log \frac{n(L_n + 1)(N_n + 1)B_n}{\tau_n}} \\ &\quad + \sum_{z \in \{0,1\}} 4\sqrt{\frac{2 \log(4/\delta)}{n_z}} \\ &\leq C \sum_{z \in \{0,1\}} \left( \frac{1}{n_z} + \frac{1}{\sqrt{n_z}} \sqrt{n^{\frac{p}{2\xi+p}} (\log n)^3} + \sqrt{\frac{\log(1/\delta)}{n_z}} \right) \end{aligned}$$

for some constant  $C > 0$  with probability at least  $1 - 2\delta$ .

Now let  $b_n = n^{-\frac{\xi}{2\xi+d}} (\log n)^{3/2}$  up to constant with  $\delta = 1/8n$  as is done in Theorem 3. Then we obtain that  $|\phi_{\tau_n}^{\text{slide}}(f) - \phi_{n, \tau_n}^{\text{slide}}(f)| = \mathcal{O}(b_n)$ . On the other hand, using the inequality  $||a - b| - |c - d|| \leq |a - c| + |b - d|$ , the second term is bounded as

$$\begin{aligned} |\phi(f) - \phi_n(f)| &= \left| |E^0 - E^1| - |E_n^0 - E_n^1| \right| \\ &\leq |E^0 - E_n^0| + |E^1 - E_n^1| \end{aligned}$$

where  $E^z = \mathbf{E}\{\mathbf{I}(f(\mathbf{X}) > 0) | Z = z\}$  and  $E_n^z = \frac{1}{n_z} \sum_{z_i=z} \mathbf{I}(f(\mathbf{x}_i) > 0)$  for  $z = 0, 1$ . Here, we note that  $|E^z - E_n^z| = \max(E^z - E_n^z, E_n^z - E^z)$ . Let  $E_{\tau_n}^z = \mathbf{E}\{\nu_{\tau_n}(f(\mathbf{X})) | Z = z\}$  and  $E_{n, \tau_n}^z = \frac{1}{n_z} \sum_{z_i=z} \nu_{\tau_n}(f(\mathbf{x}_i))$ . Then,

$$\begin{aligned} E^z - E_n^z &\leq E_{-\tau_n}^z - E_{n, \tau_n}^z \leq |E_{-\tau_n}^z - E_{n, -\tau_n}^z| + |E_{n, -\tau_n}^z - E_{n, \tau_n}^z| \\ &\leq C_1 b_n + |E_{n, -\tau_n}^z - E_{n, \tau_n}^z| \end{aligned}$$

**Table 6**

Description of datasets and corresponding hyperparameters.

Dataset	<i>Adult</i>	<i>Bank</i>	<i>Law</i>
$n_{train}/n_{test}$	36177 / 9044	32950 / 8238	21240 / 5310
$d$	41	47	11
Epochs	2000	2000	2000
Optimizer	Adam	Adam	Adam
lr	0.5	0.05	0.005
$\lambda$	(0.01, 10)	(0.01, 50)	(0.01, 100)
$\tau$	$\sim U(0.01, 0.2)$	$\sim U(0.01, 0.2)$	$\sim U(0.01, 0.2)$
$\gamma$ (UIF)	0.01	0.01	0.01

and

$$\begin{aligned} E_n^z - E^z &\leq E_{n,-\tau_n}^z - E_{\tau_n}^z \leq |E_{n,-\tau_n}^z - E_{n,\tau_n}^z| + |E_{n,\tau_n}^z - E_{\tau_n}^z| \\ &\leq |E_{n,-\tau_n}^z - E_{n,\tau_n}^z| + C_2 b_n \end{aligned}$$

 for some constant  $C_1, C_2 > 0$  by Lemmas 2 and 5 as is done in Theorem 3. Thus we have

$$\begin{aligned} |\phi(f) - \phi_{\tau_n}^{\text{slide}}(f)| &\leq C b_n + \sum_{z=0,1} |E_{n,-\tau_n}^z - E_{n,\tau_n}^z| \\ &\quad + |\phi_{n,\tau_n}^{\text{slide}}(f) - \phi_n(f)| \\ &= C b_n + \\ &\quad \sum_{z=0,1} \left| \frac{1}{n^z} \sum_{z_i=z} (v_{-\tau_n}(f(\mathbf{x}_i)) - v_{\tau_n}(f(\mathbf{x}_i))) \right| \\ &\quad + |\phi_{n,\tau_n}^{\text{slide}}(f) - \phi_n(f)| \end{aligned}$$

 for some  $C > 0$ . Dividing the above inequality by  $\tau_n$  completes the proof.  $\square$ 

## D. Implementation details

We use a DNN model with one hidden layer of size 100 with the softmax function at the output layer. For the optimizers, the Adam optimizer (Kingma and Ba (2015)) is used with scheduling the learning rates reducing by half at every 500 epochs. For the datasets, we describe the sample sizes and feature dimensions in Table 6. In addition, we introduce the hyperparameters in Table 6 with ‘‘Epochs’’ (the total number of iterations), ‘‘Optimizer’’ (the gradient descent optimization algorithm) and ‘‘lr’’ (the initial learning rate). We fix  $\gamma$  in UIF at 0.01 and choose  $\tau \sim U(0.01, 0.2)$  along with random initials.

*Evaluation measures* The balanced accuracy of a trained prediction model  $\hat{f}$  is  $(\sum_{i:y_i=-1} \mathbb{I}(\hat{f}(\mathbf{x}_i) = y_i)/n_{-1} + \sum_{i:y_i=1} \mathbb{I}(\hat{f}(\mathbf{x}_i) = y_i)/n_{1})/2$ . For the consistency (Con.), we compute the rate of predictions that do not change when only the sensitive variable is changed. That is, Con. is computed as  $\sum_{i=1}^n \mathbb{I}\{\hat{f}(\mathbf{x}_{i,z_i=0}) = \hat{f}(\mathbf{x}_{i,z_i=1})\}/n$ , where  $\mathbf{x}_{i,z_i=z}$  is an input vector which is the same as  $\mathbf{x}_i$  except  $z_i = z$ . Con. is initially considered by Yurochkin and Sun

(2020); Yurochkin et al. (2020). The S-Con. and GR-Con. in Table 4 of Section 5 are the Con. values when  $z$  is the ‘‘spouse’’ variable and the multiples of ‘‘gender’’ and ‘‘race’’ variables, respectively.

*Generating adversarial inputs for UIF* For UIF, in practice, we should compute an adversarial input  $\mathbf{x}_{adv} := \arg \max_{\mathbf{x}': d(\mathbf{x}, \mathbf{x}') \leq \epsilon} D(f(\mathbf{x}), f(\mathbf{x}'))$  of an arbitrary input  $\mathbf{x}$ . We use  $\mathbf{x}_{adv} := \mathbf{x} + \mathbf{r}_{adv}$ , where  $\mathbf{r}_{adv}$  is an adversarial direction. It is approximated by the second order Taylor’s polynomial with an approximated Hessian matrix as is proposed in VAT Miyato, ichi Maeda, Koyama and Ishii (2018). The source code that we use to generate  $\mathbf{x}_{adv}$  is a modified version of the source code from <https://github.com/lyakaap/VAT-pytorch/blob/master/vat.py>, where we replace the Kullback-Leibler divergence in VAT by the similarity metric  $D$ .

## E. Additional experiments

In this section, we present the results of additional experiments.

*An additional experiment similar to Figure 2* The 2-D dataset used in Figure 2 is generated from two Gaussians:  $\mathbf{X}|Y = 0 \sim \mathcal{N}([0.5, 4.5]^T, 2I_2)$ ,  $\mathbf{X}|Y = 1 \sim \mathcal{N}([2.0, 0.5]^T, 2I_2)$ . We did a similar experiment with the two-moon dataset illustrated in the left panel of the Figure 6. Even though the two used datasets in Figure 2 and Figure 6 are completely different, the behaviors of the Hausdorff distances are similar in the sense that the hinge-surrogate fairness constraint does not approximate the original fairness constraint well while the SLIDE works well. Note that we consider  $\alpha$  less than 0.25 since the level of fairness for the optimal classifier is around 0.25 in this two-moon dataset.

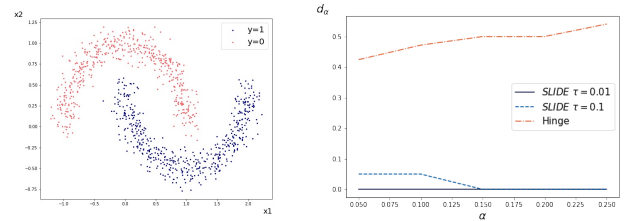


**Figure 6:** (Left) The two-moon dataset. (Right) Plot of  $\alpha$  vs.  $d_{\alpha}^{\text{hinge}}$  and  $d_{\alpha,\tau}^{\text{slide}}$  for  $\tau \in \{0.01, 0.1\}$ .

*An example of inconsistency of fairness for the hinge-surrogate fairness constraint* Let  $X \in \mathbb{R}$  be a random variable having the distribution as  $X|Z = z \sim \mathcal{N}(z, 1)$  for  $z \in \{-1, 1\}$ . For  $\mathcal{F}$ , we consider linear models as  $\mathcal{F} = \beta_0 + \beta x : \beta_0 \in [-1, 1], \beta \in [-1, 1]$ . Note that  $\beta_0 + \beta X|Z = z \sim \mathcal{N}(\beta_0 + \beta z, \beta^2)$ . Hence, the DI value for given  $(\beta_0, \beta)$  is computed by  $\text{DI}(\beta_0, \beta) = |\Phi(-\beta_0/\beta + 1) - \Phi(-\beta_0/\beta - 1)|$ , where  $\Phi(\cdot)$  is the cumulative distribution of  $\mathcal{N}(0, 1)$ . On the other hand, by formula of the mean of the truncated normal distribution, we have  $\mathbf{E}((\beta_0 + \beta \mathbf{X} + 1)_+ | Z = z) =$

**Table 7**

Average (s.e.) values  $M_{n,\hat{f}_n} \tau_n / \phi(\hat{f}_n) \times 100\%$  of the learned fair prediction models  $\hat{f}_n$ . We take the averages on random initial model parameters.

Dataset	DI + SLIDE	UIF + SLIDE
<i>Adult</i>	5.42 (4.73)	10.65 (3.69)
<i>Bank</i>	10.12 (4.90)	2.67 (0.38)
<i>Law</i>	8.17 (2.21)	8.33 (0.82)

$\beta_0 + \beta z + 1 + \frac{\phi(-(\beta_0 + \beta z + 1)/\beta)}{1 - \Phi(-(\beta_0 + \beta z + 1)/\beta)}$  where  $\phi(\cdot)$  is the probability density function of  $\mathcal{N}(0, 1)$ . Thus we have  $\text{DI}^{\text{hinge}}(\beta_0, \beta) = \left| -2\beta + \frac{\phi(-(\beta_0 - \beta + 1)/\beta)}{1 - \Phi(-(\beta_0 - \beta + 1)/\beta)} - \frac{\phi(-(\beta_0 + \beta + 1)/\beta)}{1 - \Phi(-(\beta_0 + \beta + 1)/\beta)} \right|$ . The left panel of Figure 7 draws the  $d_\alpha^{\text{hinge}}$  from  $\text{DI}^{\text{hinge}}(\beta_0, \beta)$  above, which clearly shows that the hinge-surrogate fairness constraint is not consistent in group fairness.

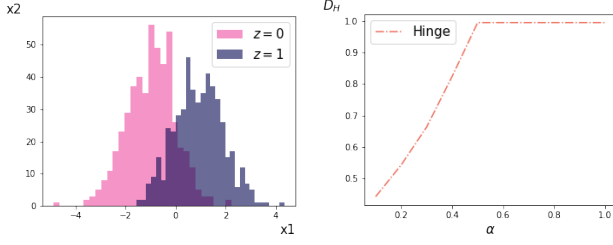


**Figure 7:** (Left) The generated dataset,  $X|Z = z \sim \mathcal{N}(z, 1)$ . (Right) Plot of  $\alpha$  vs.  $d_\alpha^{\text{hinge}}$ .

*About  $M_{n,\hat{f}_n}$*  Table 7 presents the values of  $M_{n,\hat{f}_n} \tau_n / \phi(\hat{f}_n)$  for the learned prediction models on the three datasets and two fairness criteria. Note that  $M_{n,\hat{f}_n} \tau_n$  is not much larger than 10% of  $\phi(\hat{f}_n)$  for all the cases, which confirms the validity of the SLIDE-surrogate fairness constraint.

*Simulation for Theorem 3* We perform a numerical simulation supporting Theorem 3 in Section 4, which proves that the  $l$ -excess risk  $\mathcal{E}(\hat{f}_n, f_\alpha^*)$  and the fairness risk  $\phi(\hat{f}_n) - \alpha$  converge to 0 at certain rates as the sample size increases. For simulation data, consider the following distribution:  $\mathbf{X}|S = 0, Y = 0 \sim \mathcal{N}(-1, 1.5)$ ,  $\mathbf{X}|S = 0, Y = 1 \sim \mathcal{N}(1.5, 0.5)$ ,  $\mathbf{X}|S = 1, Y = 0 \sim \mathcal{N}(-0.5, 1.0)$ , and  $\mathbf{X}|S = 1, Y = 1 \sim \mathcal{N}(2.5, 1.5)$ . We choose the DI for the fairness criterion and the linear model for the classifier. We set  $\alpha = 0.2$  and learn a fair prediction model  $\hat{f}_n$  with the SLIDE-surrogate constraint (i.e., DI + SLIDE) with  $\tau = 0.1$ . Figure 8 shows the excess risk  $\mathcal{E}(\hat{f}_n, f_\alpha^*)$  and fairness deviation  $|\phi(\hat{f}_n) - \alpha|$  for various sizes of training data. It is obvious that the two quantities become smaller as the sample size increases, which clearly confirms the validity of the results of Theorem 3.

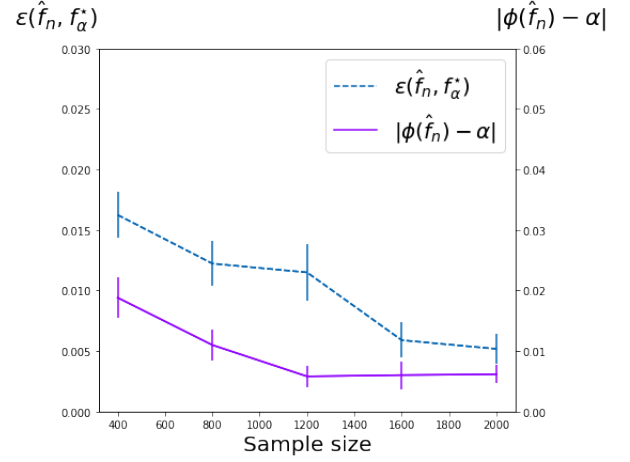


**Figure 8:** The  $l$ -excess risk  $\mathcal{E}(\hat{f}_n, f_\alpha^*)$  and the fairness deviation  $|\phi(\hat{f}_n) - \alpha|$  for various sample sizes of the training data.

**Table 8**

Comparison of UIF + {Hinge, SLIDE, HySLIDE, SLIDE (CCCP)} on *Adult*, *Bank* and *Law* test datasets.

<i>Adult</i>	Acc	BA	Con. (se)
UIF + Hinge	84.60	75.75	.918 (.003)
UIF + SLIDE	84.36	75.73	.920 (.005)
UIF + HySLIDE	84.51	75.69	<b>.922</b> (.003)
UIF + SLIDE (CCCP)	84.52	75.70	.921 (.004)
<i>Bank</i>	Acc	BA	Con. (se)
UIF + Hinge	90.29	63.82	.985 (.006)
UIF + SLIDE	90.14	63.43	<b>.990</b> (.005)
UIF + HySLIDE	90.15	63.03	.984 (.004)
UIF + SLIDE (CCCP)	90.73	63.11	.985 (.007)
<i>Law</i>	Acc	BA	Con. (se)
UIF + Hinge	83.75	62.67	.985 (.006)
UIF + SLIDE	83.99	62.71	.986 (.004)
UIF + HySLIDE	84.02	62.79	.987 (.003)
UIF + SLIDE (CCCP)	84.11	62.66	<b>.992</b> (.006)

*Application of CCCP to UIF + SLIDE* We can apply the CCCP algorithm Yuille and Rangarajan (2002) to find a local solution to the UIF + SLIDE constrained empirical risk minimization problem. The advantage of the CCCP algorithm is that it always converges to a local minimum. Note that the SLIDE function  $v_\tau$  can be decomposed to the sum of the convex function  $v_{\text{conv}}(z) = (z)_+ / \tau$  and the concave function  $v_{\text{conc}} = -(z - \tau)_+ / \tau$ . Note that we are to find a (local) minimum of  $L_n(f) + \lambda \phi_{n,\tau}^{\text{slide}}(f; \gamma, \epsilon)$ . Let  $f^{\text{curr}}$  be the current solution. Then, the CCCP algorithm updates  $f$  by minimizing

$$L_n(f) + \lambda \left\{ \phi_{n,\tau}^{\text{slide, conv}}(f; \gamma, \epsilon) + f^\top \nabla \phi_{n,\tau}^{\text{slide, conc}}(f^{\text{curr}}; \gamma, \epsilon) \right\},$$

**Table 9**

Comparison of UIF + {Hinge, SLIDE, HySLIDE, SLIDE (CCCP)} on *Adult* test dataset. For UIF + Linear and SenSR, we copied the results from Yurochkin and Sun (2020).

<i>Adult</i>	Acc	BA	S-Con.	GR-Con.
UIF + Hinge	85.3	76.8	.936	.967
UIF + SLIDE	85.1	76.6	.970	<b>.985</b>
UIF + HySLIDE	85.2	76.6	<b>.976</b>	.981
UIF + SLIDE (CCCP)	85.2	76.8	<u>.974</u>	.968
UIF + Linear (SenSel)	-	76.8	.945	.963
SenSR	78.7	78.9	.934	<u>.984</u>

where

$$\phi_{n,\tau}^{\text{slide, conv}}(f; \gamma, \epsilon) = \frac{1}{n} \sum_{i=1}^n \{D(f(\mathbf{x}_i), f(\mathbf{v}_i)) - \gamma\}_+ / \tau$$

and

$$\phi_{n,\tau}^{\text{slide, conc}}(f; \gamma, \epsilon) = -\frac{1}{n} \sum_{i=1}^n \{D(f(\mathbf{x}_i), f(\mathbf{v}_i)) - \gamma - \tau\}_+ / \tau,$$

and  $\mathbf{v}_i$  is the adversarial input of  $\mathbf{x}_i$ , that is,

$$\mathbf{v}_i = \arg \max_{\mathbf{v}; D(\mathbf{x}_i, \mathbf{v}) \leq \epsilon} D(f(\mathbf{x}_i), f(\mathbf{v})).$$

Table 8 and Table 9 are the reproductions of Table 3 and Table 4 in the main paper with adding the results of the CCCP algorithm. The results suggest that the CCCP algorithm with the SLIDE is a promising alternative to the standard gradient descent algorithm.

## References

- Agarwal, A., Beygelzimer, A., Dudik, M., Langford, J., Wallach, H., 2018. A reductions approach to fair classification, in: Dy, J., Krause, A. (Eds.), Proceedings of the 35th International Conference on Machine Learning, PMLR. pp. 60–69. URL: <https://proceedings.mlr.press/v80/agarwal18a.html>.
- Angwin, J., Larson, J., Mattu, S., Kirchner, L., 2016. Machine bias. ProPublica, May 23, 2016.
- Awasthi, P., Beutel, A., Kleindessner, M., Morgenstern, J., Wang, X., 2021. Evaluating fairness of machine learning models under uncertain and incomplete information, in: Proceedings of the 2021 ACM Conference on Fairness, Accountability, and Transparency, Association for Computing Machinery, New York, NY, USA. p. 206–214. URL: <https://doi.org/10.1145/3442188.3445884>, doi:10.1145/3442188.3445884.
- Barocas, S., Selbst, A.D., 2016. Big data’s disparate impact. California Law Review 104, 671–732. URL: <http://www.jstor.org/stable/24758720>.
- Bartlett, P.L., Jordan, M.I., McAuliffe, J.D., 2006. Convexity, classification, and risk bounds. Journal of the American Statistical Association 101, 138–156.
- Blanchard, G., Bousquet, O., Massart, P., 2008. Statistical performance of support vector machines. The Annals of Statistics 36, 489–531.
- Calders, T., Kamiran, F., Pechenizkiy, M., 2009. Building classifiers with independency constraints, in: 2009 IEEE International Conference on Data Mining Workshops, IEEE. pp. 13–18.
- Celis, L.E., Huang, L., Keswani, V., Vishnoi, N.K., 2019. Classification with fairness constraints: A meta-algorithm with provable guarantees, in: Proceedings of the Conference on Fairness, Accountability, and Transparency, pp. 319–328.
- Cho, J., Suh, C., Hwang, G., 2020. A fair classifier using kernel density estimation, in: 34th Conference on Neural Information Processing Systems, NeurIPS 2020, Conference on Neural Information Processing Systems.
- Chuang, C.Y., Mroueh, Y., 2021. Fair mixup: Fairness via interpolation, in: International Conference on Learning Representations. URL: <https://openreview.net/forum?id=DN155BXeBn>.
- Chzhen, E., Denis, C., Hebiri, M., Oneto, L., Pontil, M., 2019. Leveraging labeled and unlabeled data for consistent fair binary classification, in: Advances in Neural Information Processing Systems, pp. 12760–12770.
- Corbett-Davies, S., Pierson, E., Feller, A., Goel, S., Huq, A., 2017. Algorithmic decision making and the cost of fairness, in: Proceedings of the 23rd acm sigkdd international conference on knowledge discovery and data mining, pp. 797–806.
- Cotter, A., Jiang, H., Sridharan, K., 2019. Two-player games for efficient non-convex constrained optimization, in: ALT.
- Creager, E., Madras, D., Jacobsen, J.H., Weis, M., Swersky, K., Pitassi, T., Zemel, R., 2019. Flexibly fair representation learning by disentanglement, in: International Conference on Machine Learning, PMLR. pp. 1436–1445.
- Donini, M., Oneto, L., Ben-David, S., Shawe-Taylor, J.S., Pontil, M., 2018. Empirical risk minimization under fairness constraints, in: Advances in Neural Information Processing Systems, pp. 2791–2801.
- Dua, D., Graff, C., 2017. UCI machine learning repository. URL: <http://archive.ics.uci.edu/ml>.
- Dwork, C., Hardt, M., Pitassi, T., Reingold, O., Zemel, R., 2012. Fairness through awareness, in: Proceedings of the 3rd Innovations in Theoretical Computer Science Conference, Association for Computing Machinery, New York, NY, USA. p. 214–226. URL: <https://doi.org/10.1145/2090236.2090255>, doi:10.1145/2090236.2090255.
- Feldman, M., Friedler, S.A., Moeller, J., Scheidegger, C., Venkatasubramanian, S., 2015. Certifying and removing disparate impact, in: proceedings of the 21th ACM SIGKDD international conference on knowledge discovery and data mining, pp. 259–268.
- Fish, B., Kun, J., Lelkes, Á.D., 2016. A confidence-based approach for balancing fairness and accuracy, in: Proceedings of the 2016 SIAM International Conference on Data Mining, SIAM. pp. 144–152.
- van de Geer, S.A., 2000. Empirical processes in m-estimation.
- Goh, G., Cotter, A., Gupta, M., Friedlander, M.P., 2016. Satisfying real-world goals with dataset constraints, in: Advances in Neural Information Processing Systems, pp. 2415–2423.
- Hardt, M., Price, E., Srebro, N., 2016. Equality of opportunity in supervised learning, in: Advances in neural information processing systems, pp. 3315–3323.
- Jiang, R., Pacchiano, A., Stepleton, T., Jiang, H., Chiappa, S., 2020. Wasserstein fair classification, in: Uncertainty in Artificial Intelligence, PMLR. pp. 862–872.
- Kamiran, F., Karim, A., Zhang, X., 2012. Decision theory for discrimination-aware classification, in: 2012 IEEE 12th International Conference on Data Mining, IEEE. pp. 924–929.
- Kamishima, T., Akaho, S., Asoh, H., Sakuma, J., 2012. Fairness-aware classifier with prejudice remover regularizer, in: Joint European Conference on Machine Learning and Knowledge Discovery in Databases, Springer. pp. 35–50.
- Kingma, D.P., Ba, J., 2015. Adam: A method for stochastic optimization, in: Bengio, Y., LeCun, Y. (Eds.), 3rd International Conference on Learning Representations, ICLR 2015, San Diego, CA, USA, May 7-9, 2015, Conference Track Proceedings. URL: <http://arxiv.org/abs/1412.6980>.
- Kleinberg, J., Ludwig, J., Mullainathan, S., Rambachan, A., 2018. Algorithmic fairness, in: Aea papers and proceedings, pp. 22–27.
- Lichman, M., 2013. UCI machine learning repository. URL: <http://archive.ics.uci.edu/ml>.
- Lohaus, M., Perrot, M., Luxburg, U.V., 2020. Too relaxed to be fair, in: III, H.D., Singh, A. (Eds.), Proceedings of the 37th International Conference on Machine Learning, PMLR. pp. 6360–6369. URL: <https://proceedings.mlr.press/v119/lohaus20a.html>.
- Madras, D., Creager, E., Pitassi, T., Zemel, R.S., 2018. Learning adversarially fair and transferable representations, in: ICML.

- Mahendhiran, P., Subramanian, K., 2018. Deep learning techniques for polarity classification in multimodal sentiment analysis. *International Journal of Information Technology and Decision Making* 17. doi:10.1142/S0219622018500128.
- Maity, S., Xue, S., Yurochkin, M., Sun, Y., 2021. Statistical inference for individual fairness. URL: <https://arxiv.org/abs/2103.16714>, doi:10.48550/ARXIV.2103.16714.
- Mehrabi, N., Morstatter, F., Saxena, N., Lerman, K., Galstyan, A., 2019. A survey on bias and fairness in machine learning. arXiv preprint arXiv:1908.09635 .
- Miyato, T., Ichi Maeda, S., Koyama, M., Ishii, S., 2018. Virtual adversarial training: A regularization method for supervised and semi-supervised learning. arXiv:1704.03976.
- Pleiss, G., Raghavan, M., Wu, F., Kleinberg, J., Weinberger, K.Q., 2017. On fairness and calibration, in: *Advances in Neural Information Processing Systems*, pp. 5680–5689.
- Schmidt-Hieber, J., et al., 2020. Nonparametric regression using deep neural networks with relu activation function. *Annals of Statistics* 48, 1875–1897.
- Shalev-Shwartz, S., Ben-David, S., 2014. *Understanding machine learning: From theory to algorithms*. Cambridge university press.
- Shen, X., Tseng, G.C., Zhang, X., Wong, W.H., 2003. On  $\psi$ -learning. *Journal of the American Statistical Association* 98, 724–734.
- Suzuki, T., 2019. Adaptivity of deep reLU network for learning in besov and mixed smooth besov spaces: optimal rate and curse of dimensionality, in: *International Conference on Learning Representations*. URL: <https://openreview.net/forum?id=H1ebTsActm>.
- Vogel, R., Bellet, A., Cléménçon, S., 2020. Learning Fair Scoring Functions: Fairness Definitions, Algorithms and Generalization Bounds for Bipartite Ranking. arXiv preprint arXiv:2002.08159 .
- Webster, K., Recasens, M., Axelrod, V., Baldrige, J., 2018. Mind the gap: A balanced corpus of gendered ambiguous pronouns. *Transactions of the Association for Computational Linguistics* 6, 605–617.
- Wei, D., Ramamurthy, K.N., Calmon, F., 2020. Optimized score transformation for fair classification, PMLR, Online. pp. 1673–1683. URL: <http://proceedings.mlr.press/v108/wei20a.html>.
- Wolf, M.M., 2018. *Mathematical foundations of supervised learning*.
- Woodworth, B., Gunasekar, S., Ohannessian, M.I., Srebro, N., 2017. Learning non-discriminatory predictors, in: Kale, S., Shamir, O. (Eds.), *Proceedings of the 2017 Conference on Learning Theory*, PMLR. pp. 1920–1953. URL: <http://proceedings.mlr.press/v65/woodworth17a.html>.
- Wu, Y., Zhang, L., Wu, X., 2019. On convexity and bounds of fairness-aware classification, in: *The World Wide Web Conference, Association for Computing Machinery, New York, NY, USA*. p. 3356–3362. URL: <https://doi.org/10.1145/3308558.3313723>, doi:10.1145/3308558.3313723.
- Xu, D., Yuan, S., Zhang, L., Wu, X., 2018. Fairgan: Fairness-aware generative adversarial networks, in: *2018 IEEE International Conference on Big Data (Big Data)*, IEEE. pp. 570–575.
- Yona, G., Rothblum, G., 2018. Probably approximately metric-fair learning, in: Dy, J., Krause, A. (Eds.), *Proceedings of the 35th International Conference on Machine Learning*, PMLR, Stockholm, Sweden. pp. 5680–5688.
- Yuille, A.L., Rangarajan, A., 2002. The concave-convex procedure (cccp), in: Dietterich, T., Becker, S., Ghahramani, Z. (Eds.), *Advances in Neural Information Processing Systems*, MIT Press. pp. 1033–1040.
- Yurochkin, M., Bower, A., Sun, Y., 2020. Training individually fair ml models with sensitive subspace robustness, in: *International Conference on Learning Representations*. URL: <https://openreview.net/forum?id=B1gdkxHFDH>.
- Yurochkin, M., Sun, Y., 2020. Sensei: Sensitive set invariance for enforcing individual fairness. arXiv:2006.14168.
- Zafar, M.B., Valera, I., Gomez-Rodriguez, M., Gummadi, K.P., 2019. Fairness Constraints: A Flexible Approach for Fair Classification. *J. Mach. Learn. Res.* 20, 1–42.
- Zafar, M.B., Valera, I., Rogriguez, M.G., Gummadi, K.P., 2017. Fairness constraints: Mechanisms for fair classification, in: *Artificial Intelligence and Statistics*, pp. 962–970.
- Zemel, R., Wu, Y., Swersky, K., Pitassi, T., Dwork, C., 2013. Learning fair representations, in: *International Conference on Machine Learning*, pp. 325–333.
- Zhang, T., 2004. Statistical behavior and consistency of classification methods based on convex risk minimization. *The Annals of Statistics* 32, 56–85.